The Plant Cell, Vol. 21: 2928–2947, September 2009, www.plantcell.org

In Planta Expression Screens of *Phytophthora infestans* RXLR Effectors Reveal Diverse Phenotypes, Including Activation of the *Solanum bulbocastanum* Disease Resistance Protein Rpi-blb2 [W]

Sang-Keun Oh,[a,b] Carolyn Young,[a,1] Minkyoung Lee,[a] Ricardo Oliva,[c] Tolga O. Bozkurt,[c] Liliana M. Cano,[c] Joe Win,[c] Jorunn I.B. Bos,[c] Hsin-Yin Liu,[a] Mireille van Damme,[c] William Morgan,[d] Doil Choi,[b] Edwin A.G. Van der Vossen,[e] Vivianne G.A.A. Vleeshouwers,[e] and Sophien Kamoun[a,c,2]

[a] Department of Plant Pathology, Ohio State University-Ohio Agricultural Research and Development Center, Wooster, Ohio 44691

[b] Department of Plant Sciences, College of Agriculture and Life Sciences, Seoul National University, Seoul 151-742, Korea

[c] The Sainsbury Laboratory, Norwich NR4 7UH, United Kingdom

[d] Department of Biology, The College of Wooster, Wooster, Ohio 44691

[e] Wageningen UR Plant Breeding, 6700 AJ Wageningen, The Netherlands

The Irish potato famine pathogen *Phytophthora infestans* is predicted to secrete hundreds of effector proteins. To address the challenge of assigning biological functions to computationally predicted effector genes, we combined allele mining with high-throughput in planta expression. We developed a library of 62 infection-ready *P. infestans* RXLR effector clones, obtained using primer pairs corresponding to 32 genes and assigned activities to several of these genes. This approach revealed that 16 of the 62 examined effectors cause phenotypes when expressed inside plant cells. Besides the well-studied AVR3a effector, two additional effectors, PexRD8 and PexRD36$_{45\text{-}1}$, suppressed the hypersensitive cell death triggered by the elicitin INF1, another secreted protein of *P. infestans*. One effector, PexRD2, promoted cell death in *Nicotiana benthamiana* and other solanaceous plants. Finally, two families of effectors induced hypersensitive cell death specifically in the presence of the *Solanum bulbocastanum* late blight resistance genes *Rpi-blb1* and *Rpi-blb2*, thereby exhibiting the activities expected for *Avrblb1* and *Avrblb2*. The AVRblb2 family was then studied in more detail and found to be highly variable and under diversifying selection in *P. infestans*. Structure-function experiments indicated that a 34–amino acid region in the C-terminal half of AVRblb2 is sufficient for triggering Rpi-blb2 hypersensitivity and that a single positively selected AVRblb2 residue is critical for recognition by Rpi-blb2.

INTRODUCTION

Our understanding of the pathogenicity mechanisms of filamentous microbes, such as oomycetes and fungi, has been limited mainly to the development of specialized infection structures, secretion of hydrolytic enzymes, production of host selective toxins, and detoxification of plant antimicrobial compounds (Idnurm and Howlett, 2001; Talbot, 2003; Randall et al., 2005). Recent findings, however, significantly broadened our view of pathogenicity to reveal that filamentous pathogens are much more sophisticated manipulators of plant cells than previously anticipated. Indeed, similar to bacterial pathogens, eukaryotic pathogens secrete an arsenal of proteins, termed effectors, that modulate plant innate immunity and enable parasitic colonization and reproduction (Birch et al., 2006; Chisholm et al., 2006; Kamoun, 2006; O'Connell and Panstruga, 2006; Catanzariti et al., 2007; Kamoun, 2007). Although effectors are thought to function primarily in virulence, they can also elicit innate immunity in plant varieties that carry cognate disease resistance (R) proteins. In such cases, effectors are said to have an avirulence (Avr) activity, thereby activating directly or indirectly programmed cell death (hypersensitive response [HR]) and associated resistance responses mediated by specific R proteins. Deciphering the virulence and avirulence activities of effectors to understand how pathogens interact and coevolve with their host plants has become a driving research paradigm in the field of oomycete and fungal pathology. In particular, the recent availability of genome-wide catalogs of effector secretomes from dozens of filamentous pathogen genome sequences calls for high-throughput approaches (effectoromics) to rapidly and efficiently assign functions to computationally predicted effector genes.

The oomycetes form a phylogenetically distinct group of eukaryotic microorganisms that includes some of the most destructive pathogens of plants (Kamoun, 2003). The most

[1] Current address: The Samuel Roberts Noble Foundation, Ardmore, OK 73401.

[2] Address correspondence to sophien.kamoun@tsl.ac.uk.

The author responsible for distribution of materials integral to the findings presented in this article in accordance with the policy described in the Instructions for Authors (www.plantcell.org) is: Sophien Kamoun (sophien.kamoun@tsl.ac.uk).

[W] Online version contains Web-only data.

www.plantcell.org/cgi/doi/10.1105/tpc.109.068247

notorious oomycete is the potato (*Solanum tuberosum*) and tomato (*Solanum lycopersicum*) late blight pathogen *Phytophthora infestans*. A pathogen of historical significance as the cause of the Irish potato famine, *P. infestans* not only continues to cost modern agriculture billions of dollars annually but also impacts subsistence farming in developing countries (Kamoun and Smart, 2005; Fry, 2008). *P. infestans* is a hemibiotrophic pathogen that initially requires living host cells but then causes extensive necrosis of host tissue culminating in profuse sporulation (Kamoun and Smart, 2005). During the biotrophic phase, the pathogen establishes intimate associations with host cells through the production of digit-like haustoria, structures that function in host translocation of effector proteins and probably nutrient uptake (Birch et al., 2006; Whisson et al., 2007).

Like other oomycetes, *P. infestans* is predicted to secrete hundreds of effector proteins that target two distinct sites in the host plant (Kamoun, 2006; Whisson et al., 2007; Haas et al., 2009). Apoplastic effectors are secreted into the plant extracellular space, whereas cytoplasmic effectors are translocated into the plant cell, where they target different subcellular compartments. In contrast with apoplastic effectors, which are known to inhibit host hydrolases (Tian et al., 2004, 2005, 2007; Damasceno et al., 2008), the biochemical activities of cytoplasmic effectors remain poorly understood. Oomycete cytoplasmic effectors are modular proteins that carry N-terminal signal peptides followed by conserved motifs, notably the RXLR and LXLFLAK motifs (Birch et al., 2006; Kamoun, 2006; Tyler et al., 2006; Kamoun, 2007; Morgan and Kamoun, 2007; Win et al., 2007; Birch et al., 2008). The RXLR motif defines a domain, similar to a host translocation signal of malaria parasites, that enables delivery of effector proteins inside plant cells (Bhattacharjee et al., 2006; Whisson et al., 2007; Dou et al., 2008b; Grouffaud et al., 2008). One of the best-studied oomycete RXLR effectors is *P. infestans* AVR3a, which confers avirulence on potato plants carrying the *R3a* gene (Armstrong et al., 2005). In addition to its avirulence activity, AVR3a suppresses the cell death induced by INF1 elicitin, another secreted protein of *P. infestans* with features of pathogen-associated molecular patterns (PAMPs) (Bos et al., 2006, 2009). AVR3a is thought to contribute to virulence through this PAMP suppression activity (Bos et al., 2009).

More than a dozen late blight resistance genes (*R* genes) have been introgressed into cultivated potato from wild species such as *Solanum demissum*, *Solanum bulbocastanum*, and *Solanum berthaultii* using classical breeding (Fry, 2008). Some of these *R* genes, notably *S. demissum R1* and *R3a* as well as *S. bulbocastanum Rpi-blb1* (also known as *RB*) and *Rpi-blb2*, have been cloned (Ballvora et al., 2002; Song et al., 2003; van der Vossen et al., 2003, 2005; Huang et al., 2005; Kuang et al., 2005; Vleeshouwers et al., 2008; Wang et al., 2008). Although late blight *R* genes have long been noted to be ineffective in the field over long periods of time, empirical observations backed by plausible hypotheses indicate that some of the newly cloned *R* genes could mediate resistance in a durable enough fashion to prove useful in agriculture (Helgeson et al., 1998; Song et al., 2003; van der Vossen et al., 2003, 2005). For example, *Rpi-blb1* recognizes a broad spectrum of *P. infestans* isolates and has proven effective in the field in several geographical areas and over several growing seasons (Helgeson et al., 1998; Song et al., 2003; van der Vossen et al., 2003; Kuhl et al., 2007; Halterman et al., 2008). This has prompted interest in the deployment of potato cultivars with these novel *R* genes. A transgenic potato variety carrying *Rpi-blb1* and *Rpi-blb2* has entered the commercialization pipeline in Europe (Vleeshouwers et al., 2008), and other initiatives to release these genes in several developing countries are under way (USAID Agricultural Biotechnology Support Project II, http://www.absp2.cornell.edu). The identification of the *Avr* genes targeted by these *R* genes would help to determine the extent to which broad-spectrum resistance differs from other types of resistance and will generate the tools to monitor *P. infestans* populations for mutations in the *Avr* genes (Kamoun and Smart, 2005; Vleeshouwers et al., 2008).

The discovery that oomycete AVR proteins belong to the RXLR effector class creates the opportunity to use bioinformatics to predict a robust set of candidate effectors. In this study, we combined allele mining with high-throughput in planta expression to assess the activities of 62 RXLR effector homologs from *P. infestans*. This effectoromics approach revealed that 16 of the 62 effectors cause phenotypes when expressed in planta. Four distinct effector activities were observed: (1) suppression of INF1 triggered cell death, (2) nonspecific induction of weak cell death response in *Nicotiana benthamiana* and other solanaceous plants, (3) specific induction of HR cell death in the presence of *Rpi-blb1*, and (4) specific induction of HR cell death in the presence of *Rpi-blb2*. The latter two activities are expected for *Avrblb1* and *Avrblb2*. The AVRblb2 family was then studied in more detail revealing that a single amino acid site under positive selection in *P. infestans* is critical for recognition by Rpi-blb2. A subset of the infection-ready library we describe here was previously used to screen a collection of *Solanum* genotypes for induction of HR-like symptoms and resulted in the independent discovery of *Avrblb1* (Vleeshouwers et al., 2008).

RESULTS

Strategy for Allele Mining and in Planta Expression of *P. infestans* RXLR Effectors

To identify RXLR effectors with novel activities, we devised a strategy that combines allele mining with in planta expression (Figure 1). In brief, primer pairs based on the mature region of candidate RXLR effectors (without the signal peptide) were designed and used to amplify genomic DNA from a panel of *P. infestans* isolates. All amplicons were sequenced to reveal whether or not the examined gene is polymorphic. Mixed amplicons were frequently observed as previously noted in *P. infestans* and are the result of either heterozygosity or closely related paralogs (Bos et al., 2003; Armstrong et al., 2005; Liu et al., 2005). Amplicons deemed to be novel in sequence were prioritized for cloning into the *Agrobacterium tumefaciens* binary *Potato virus X* (PVX) vector pGR106, which enables high-throughput screening in planta (Lu et al., 2003; Huitema et al., 2004). Clone inserts were sequenced to yield a library of nonredundant clones. A microplate was assembled with the collection of nonredundant clones and used as a template for in planta expression to assay for cell death elicitation and suppression as well as avirulence activity by coexpression with specific *R* genes.

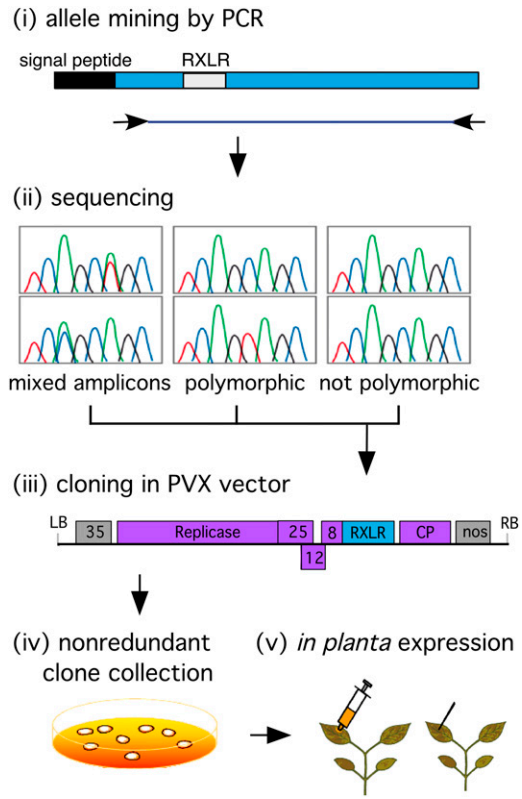

Figure 1. Overview of the Effectoromics Pipeline for Allele Mining, Cloning, and in Planta Expression of RXLR Effectors.

The various steps in the pipeline are as follows: (1) PCR-based allele mining using primers designed to amplify sequences corresponding to the mature RXLR proteins and including an in-frame ATG start codon. (2) Sequencing of amplicons and prioritization for cloning. (3) Cloning of amplicons in the PVX-based expression vector pGR106. (4) Transformation of constructs into *A. tumefaciens* GV3101 and sequencing of inserts to yield a library of nonredundant clones. (5) Testing mutants of interest for suppression and promotion of cell death, as well as for specific activation of *R* genes, by agroinfiltration and wound inoculation in *N. benthamiana*.

An Infection-Ready Collection of 62 *P. infestans* RXLR Effectors (*PexRD* Genes)

We successfully implemented the strategy described above using primers corresponding to a total of 32 candidate RXLR effector genes (see Supplemental Table 1 online) and a panel of up to 26 isolates of *P. infestans* from the US and The Netherlands (see Supplemental Table 2 online). The genes, named *PexRD1* to *PexRD50* (Table 1), were selected for the most part prior to the completion of the genome sequence of *P. infestans* T30-4 strain (Haas et al., 2009) and were mined from a large collection of >80,000 ESTs generated from several *P. infestans* developmental and infection stages (Randall et al., 2005). A collection of 62 nonredundant RXLR effectors, representing the 32 *PexRD* genes, were identified following cloning in the PVX vector pGR106 (Table 1; full description in Supplemental Data Set 1 online). We determined that 53 of the 62 sequences could be grouped in 15 families with 2 to 21 sequences per family (see Supplemental Table 3 online). Because closely related sequences could correspond to either alleles or paralogs, we will refer to them as homologs.

Over Half the Examined RXLR Effector Genes Are Polymorphic

Of the 32 *PexRD* genes examined, 18 (56%) turned out to be polymorphic among the examined *P. infestans* isolates (Table 1). Of these, 13 genes displayed nonsynonymous amino acid polymorphisms, four had premature stop codons when compared with the parental EST, whereas one gene had only silent mutations (synonymous amino acid substitutions). These results are consistent with the rapid evolutionary rates associated with RXLR effectors (Tyler et al., 2006; Win et al., 2007) and also indicate that the majority of the observed polymorphisms are expected to be functionally relevant. As reported earlier in a genome-wide analysis of RXLR effector paralogs of *Phytophthora sojae*, *Phytophthora ramorum*, and *Hyaloperonospora arabidopsidis* (Win et al., 2007), most of the polymorphisms localized to the C-terminal region of the effectors, and the RXLR and EER motifs were invariably conserved across the homologs (Table 1; see Supplemental Data Set 1 online).

The Majority of the Selected RXLR Effector Genes Are Expressed during Infection of Tomato

To determine the extent to which the *P. infestans PexRD* genes are expressed during colonization of plants, we analyzed the expression of the 32 genes during the interaction of *P. infestans* with its host plant tomato using RT-PCR analyses (see Supplemental Figure 1 online). Total RNA was isolated from leaves of tomato 0, 1, 2, 3, 4, and 5 d after inoculation (DAI) with two different *P. infestans* isolates, 90128 and 88069, and from *P. infestans* mycelium grown in vitro. The constitutive elongation factor 2 alpha (*ef2a*) (Torto et al., 2002) and the in planta–induced Kazal-like protease inhibitor gene *epi1* (Tian et al., 2004) were used as controls. We detected transcripts for 30 of the 32 genes in at least one of the examined stages (see Supplemental Figure 1 online). Among these, 29 genes were expressed during colonization of tomato, whereas transcripts for *PexRD4* were detected only in mycelium (see Supplemental Figure 1 online). Transcripts for nine genes, *PexRD3*, *PexRD6/ipiO*, *PexRD8*, *PexRD24*, *PexRD31*, *PexRD44*, *PexRD45*, *PexRD49*, and *PexRD50*, were detected in the infection time points but not in mycelium (see Supplemental Figure 1 online; summarized in Table 1). These results show that the great majority of the selected RXLR effector candidate genes are expressed during infection of tomato, consistent with their predicted function.

In addition, we cross-checked our gene list with the RXLR effector genes previously reported to be induced during infection of potato using real-time PCR (Whisson et al., 2007) or using Nimblegen oligonucleotide microarrays (Haas et al., 2009). Of the 32 *PexRD* genes, 22 were shown by Whisson et al. (2007) and 16 by Haas et al. (2009) to be induced during infection of potato (see Supplemental Table 4 online). These expression data

Table 1. Description of the Selected *PexRD* Genes

Gene Name(s)	Number of Homologs Amplified	Type of Mutations	SignalP HMM Probability[a]	SignalP NN Mean S Score[a]	SignalP Length[a]	RXLR	dEER	Expression in Vitro (Mycelium)	Expression in Tomato (Infection)
PexRD1	1	None detected	0.989	0.654	19	RQLR	EDGEER	+	+
PexRD2	1	None detected	0.998	0.913	20	RLLR	ENDDDSEAR	+	+
PexRD3	1	None detected	0.998	0.741	23	RFLR	EGDNEER	−	+
PexRD4	1	None detected	0.998	0.813	21	RFLR	DEER	+	−
PexRD6, *ipiO, Avrblb1*	3	Nonsynonymous	1.000	0.968	21	RSLR	DEER	−	+
PexRD7, *Avr3a*	2	Nonsynonymous	0.998	0.745	21	RLLR	EENEETSEER	+	+
Pex147-2, *Avr3a* paralog	1	None detected	0.991	0.725	21	RLLR	EESEETSEER	−	−
Pex147-3, *Avr3a* paralog	1	None detected	0.992	0.742	21	RFLR	EENEETSEER	−	−
PexRD8	1	None detected	0.989	0.832	22	RLLR	DDDDEEER	−	+
PexRD10	1	None detected	0.998	0.925	19	RKLR	EER	+	+
PexRD11	2	Premature stop	1.000	0.907	21	RLLR	DEGELTEER	+	+
PexRD12	2	Synonymous	1.000	0.869	22	RSLR	DSDDGEER	+	+
PexRD13	2	Premature stop	1.000	0.843	21	RQLR		+	+
PexRD14	2	Nonsynonymous	1.000	0.781	23	RLLR	ETGNQEER	+	+
PexRD16	2	Nonsynonymous	1.000	0.951	20	RSLR	EER	+	+
PexRD17	2	Nonsynonymous	0.960	0.525	28	RVLR	EIEAETER	+	+
PexRD21	1	None detected	0.993	0.921	21	RLLR	EREVQEER	+	+
PexRD22	2	Nonsynonymous	0.998	0.918	17	RFLR	EDASDEER	+	+
PexRD24	2	Nonsynonymous	1.000	0.901	22	RSLR	ETSEDEEER	−	+
PexRD26	2	Nonsynonymous	0.981	0.890	22	RVLR	DEER	+	+
PexRD27	1	None detected	0.992	0.885	28	RLLR	DSEER	+	+
PexRD28	1	None detected	0.999	0.916	24	RSLR	ETSEDEEER	+	+
PexRD31	1	None detected	0.986	0.672	28	RSLR	EDQEGDEER	−	+
PexRD36	2	Premature stop	0.999	0.881	22	RHLR	DDEER	+	+
PexRD39, *Avrblb2*	13[b]	Nonsynonymous	1.000	0.864	22	RSLR		+	+
PexRD40, *Avrblb2*	13[b]	Nonsynonymous	1.000	0.857	22	RSLR		+	+
PexRD41	3	Nonsynonymous	1.000	0.849	21	RSLR		+	+
PexRD44	1	None detected	1.000	0.949	21	RFLR	QEEGVFEER	−	+
PexRD45	2	Premature stop	0.999	0.782	22	RSLR		−	+
PexRD46	3	Nonsynonymous	1.000	0.854	21	RSLR		+	+
PexRD49	1	None detected	1.000	0.924	20	RLLR	EEER	−	+
PexRD50	2	Nonsynonymous	1.000	0.875	20	RLLR		−	+

[a]S-mean value, HMM score, and signal peptide length predicted using SignalPv2.0 (http://www.cbs.dtu.dk/services/SignalP-2.0).
[b]Primers for both *PexRD39* and *PexRD40* amplified the same homologs.

independently confirm the in planta (tomato and potato) expression pattern for 27 out of the 32 candidate RXLR effector genes.

Functional Validation of the Signal Peptides of RXLR Effectors

To validate functionally the signal peptide predictions of the selected RXLR effector genes, we used a genetic assay based on the requirement of yeast cells for invertase secretion to grow on sucrose or raffinose media (Klein et al., 1996; Jacobs et al., 1997; Lee et al., 2006). The predicted signal peptide sequences and the subsequent two amino acids of four PEXRD genes, *PexRD6/ipiO*, *PexRD8*, *PexRD39*, and *PexRD40*, were fused in frame to the mature sequence of yeast invertase in the vector pSUC2 (Jacobs et al., 1997) (see Supplemental Table 5 online). All four *PexRD* constructs enabled the invertase mutant yeast strain YTK12 to grow on YPRAA medium (with raffinose instead of sucrose, growth only when invertase is secreted) (Figure 2). In addition, invertase secretion was confirmed with an enzymatic activity test based on reduction of the dye 2,3,5-triphenyltetrazolium chloride (TTC) to the insoluble red colored triphenylformazan (Figure 2). By contrast, the negative control yeast strains did not grow on YPRAA, and the TTC-treated culture filtrates remained colorless (Figure 2). These results indicate that the signal peptides of *PexRD6/ipiO*, *PexRD8*, *PexRD39*, and *PexRD40* are functional and confirm earlier observations that predictions obtained with the SignalP program are highly accurate (Menne et al., 2000; Schneider and Fechner, 2004; Lee et al., 2006).

PexRD8 and PexRD36$_{45\text{-}1}$ Suppress the Hypersensitive Cell Death Induced by INF1

Suppression of plant innate immunity, particularly PAMP-triggered immunity, has emerged as a common function of phytopathogen effectors (Block et al., 2008; Hogenhout et al., 2009). Elicitins are structurally conserved proteins in oomycetes that trigger defenses in a variety of solanaceous plants and have features of PAMPs (Nurnberger and Brunner, 2002; Vleeshouwers et al., 2006). Previously, we showed that the *P. infestans*

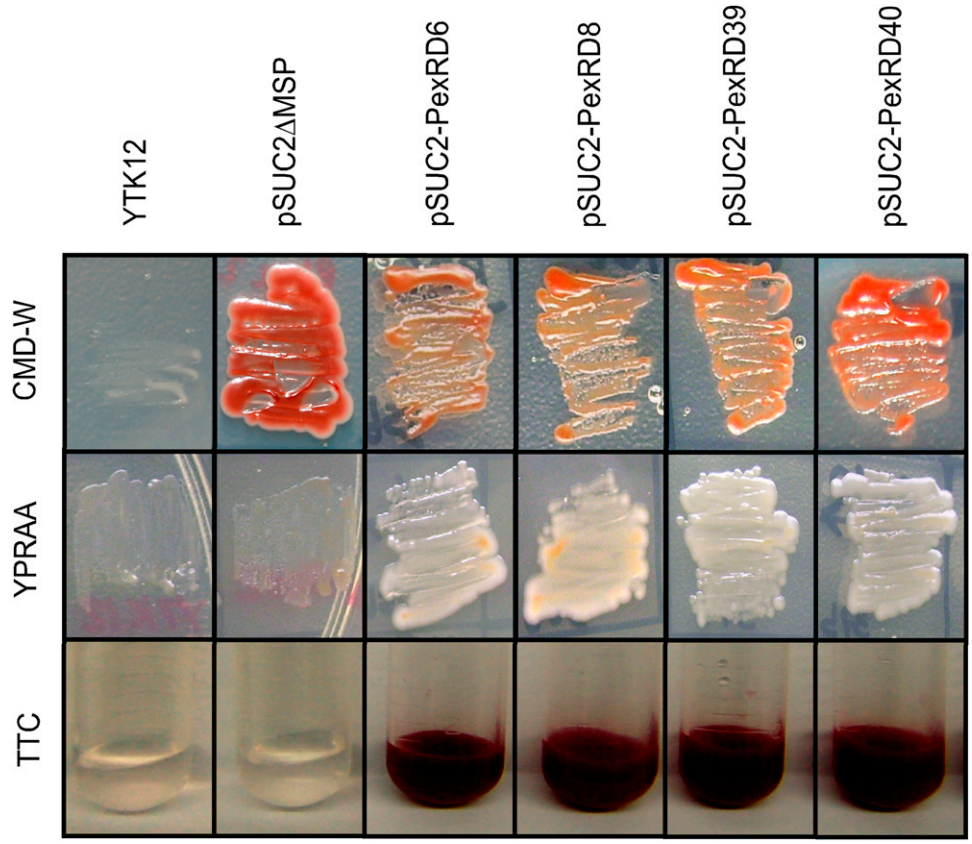

Figure 2. Functional Validation of the Signal Peptides of RXLR Effectors.

Functional validation of the signal peptides of PexRD6/IpiO, PexRD8, PexRD39, and PexRD40 was performed using the yeast invertase secretion assay. Yeast YTK12 strains carrying the PexRD signal peptide fragments fused in frame to the invertase gene in the pSUC2 vector are able to grow in both the CMD-W media (with sucrose, yeast growth even in the absence of invertase secretion) and YPRAA media (with raffinose instead of sucrose, growth only when invertase is secreted), as well as reduce TTC to red formazan, indicating secretion of invertase. The controls include the untransformed YTK12 strain and YTK12 carrying the pSUC2 vector.

RXLR effector AVR3a suppresses the cell death induced by INF1 elicitin in *N. benthamiana* (Bos et al., 2006, 2009). To identify other RXLR effectors that suppress INF1 cell death, we infiltrated *A. tumefaciens* strains carrying the 62 pGR106-PexRD constructs and the negative control pGR106-ΔGFP (for green fluorescent protein) in *N. benthamiana* leaves to express the candidate suppressors. One day later, the infiltration sites were challenged with an *A. tumefaciens* strain carrying the p35S-INF1 construct, and cell death symptoms were scored 3 to 5 d later. Phenotypic evaluation of the infiltrated sites revealed that two clones, pGR106-PexRD8 and pGR106-PexRD36$_{45\text{-}1}$, reduced the rate of INF1 cell death to below 50% compared with >90% for the control pGR106-ΔGFP and <15% for pGR106- AVR3a^{KI} (see Supplemental Figure 2 online).

To validate the results of the screen, we performed additional side-by-side assays to compare the suppression activities of PexRD8 and PexRD36$_{45\text{-}1}$ to that of AVR3a^{KI} (Figure 3). These results confirmed that PexRD8 and PexRD36$_{45\text{-}1}$ consistently suppress the HR induced by INF1, although not to the level achieved by AVR3a^{KI}. We conclude that PexRD8 and PexRD36$_{45\text{-}1}$ carry INF1 cell death suppression activity.

We also screened our pGR106-PexRD library for suppression of the necrosis induced by the *P. infestans* Nep1-like protein NPP1.1, a protein that appears to function as a toxin during the necrotrophic phase of the infection (Kanneganti et al., 2006; Qutob et al., 2006). None of the 62 clones reproducibly suppressed NPP1.1-mediated necrosis (data not shown).

PexRD2 Induces a Weak Cell Death Response in *N. benthamiana*

Ectopic expression of effector genes in plant cells often leads to macroscopic phenotypes such as cell death, chlorosis, and tissue browning when expressed in host cells (Kjemtrup et al., 2000; Torto et al., 2003; Cunnac et al., 2009; Gurlebeck et al., 2009; Haas et al., 2009). To identify *PexRD* genes that induce phenotypic symptoms in plants, we individually inoculated the *A. tumefaciens* strains carrying the 62 pGR106-PexRD plasmids on *N. benthamiana* using both the wounding (toothpick) and agroinfiltration assays (Huitema et al., 2004; Bos et al., 2009). Only pGR106-PexRD2 induced a weak delayed necrotic response appearing at 7 to 10 DAI in the toothpick assay (Figure 4A). In

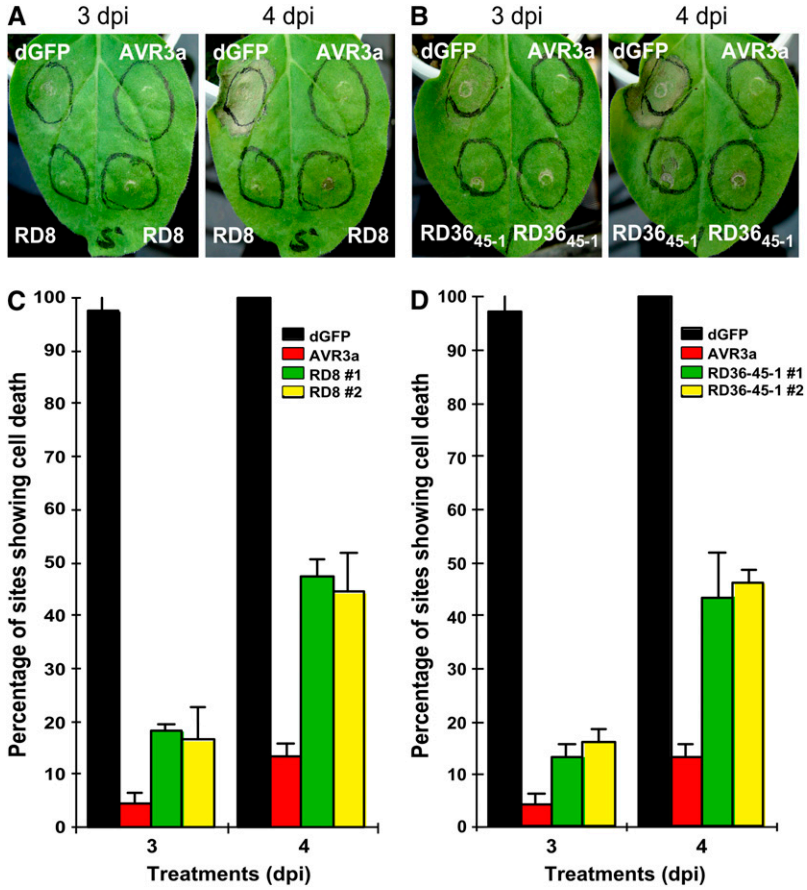

Figure 3. PexRD8 and PexRD36$_{45-1}$ Suppress the HR Induced by *P. infestans* INF1 Elicitin.

(A) and **(B)** Agroinfiltration sites in *N. benthamiana* leaves expressing either PexRD8 **(A)** or PexRD36$_{45-1}$ **(B)** were challenged with *A. tumefaciens* expressing the INF1 elicitin. The INF1-induced cell death was scored at 3 and 4 DAI. Two independent pGR106-derived clones of PexRD8 and PexRD36$_{45-1}$ were used (bottom panels; clone #1 on the bottom left side and #2 on the bottom right). *A. tumefaciens* strain carrying pGR106-ΔGFP (dGFP) was used as a negative control, and pGR106-AVR3a (AVR3a) was used as a positive control.

(C) and **(D)** Quantification of suppression of INF1 cell death by PexRD8 and PexRD36$_{45-1}$ relative to AVR3a. The mean percentages of sites showing cell death and the standard errors were scored from 20 infiltration sites based on three independent experiments using *N. benthamiana* leaves expressing either PexRD8 **(C)** or PexRD36$_{45-1}$ **(D)**. Two independent pGR106-derived clones of PexRD8 and PexRD36$_{45-1}$ were used (#1 and #2) as shown in **(A)** and **(B)**.

addition, the necrotic area was reduced relative to the HR induced by the positive control pGR106-INF1 (Figure 4A).

To determine whether enhanced expression of PexRD2 results in enhanced cell death inducing activity, we coexpressed the pGR106-PexRD2 construct with a construct expressing p19, a suppressor of posttranscriptional gene silencing from *Tomato bushy stunt virus* that is known to increase gene expression in the agroinfiltration assay (Voinnet et al., 2003). We observed that 3 to 5 d after infiltration, the PexRD2-associated cell death was accelerated and enhanced in the presence of p19 (Figure 4B). We conclude that the cell death induced by PexRD2 is probably dose dependent.

The ubiquitin ligase-associated protein SGT1 is required for a variety of cell death responses in plants (Austin et al., 2002; Azevedo et al., 2002; Peart et al., 2002; Kanneganti et al., 2006). We tested whether SGT1 is required for PexRD2-induced cell death using virus-induced gene silencing (VIGS) with *Tobacco rattle virus* (TRV) followed by agroinfiltration assays (Huitema et al., 2004). SGT1-silenced and control plants were infiltrated with *A. tumefaciens* strains containing pGR106-PexRD2 mixed with (+) p19 or without (−) p19 (Figures 4C and 4D). Silencing of SGT1 suppressed the cell death response induced by PexRD2, indicating that similar to a variety of other effectors, PexRD2 requires SGT1 to elicit cell death in *N. benthamiana*.

Functional Identification of *Avrblb1* and *Avrblb2*

We next used the PVX-based high-throughput assay to identify the *Avr* genes matching the *S. bulbocastanum R* genes *Rpi-blb1* and *Rpi-blb2* (van der Vossen et al., 2003, 2005). First, we infiltrated leaves of *N. benthamiana* with *A. tumefaciens* strains carrying one of the two *R* genes. Two days later, the leaves were wound inoculated in triplicate with each of the 62 pGR106-PexRD *A. tumefaciens* strains. The hypersensitive cell death

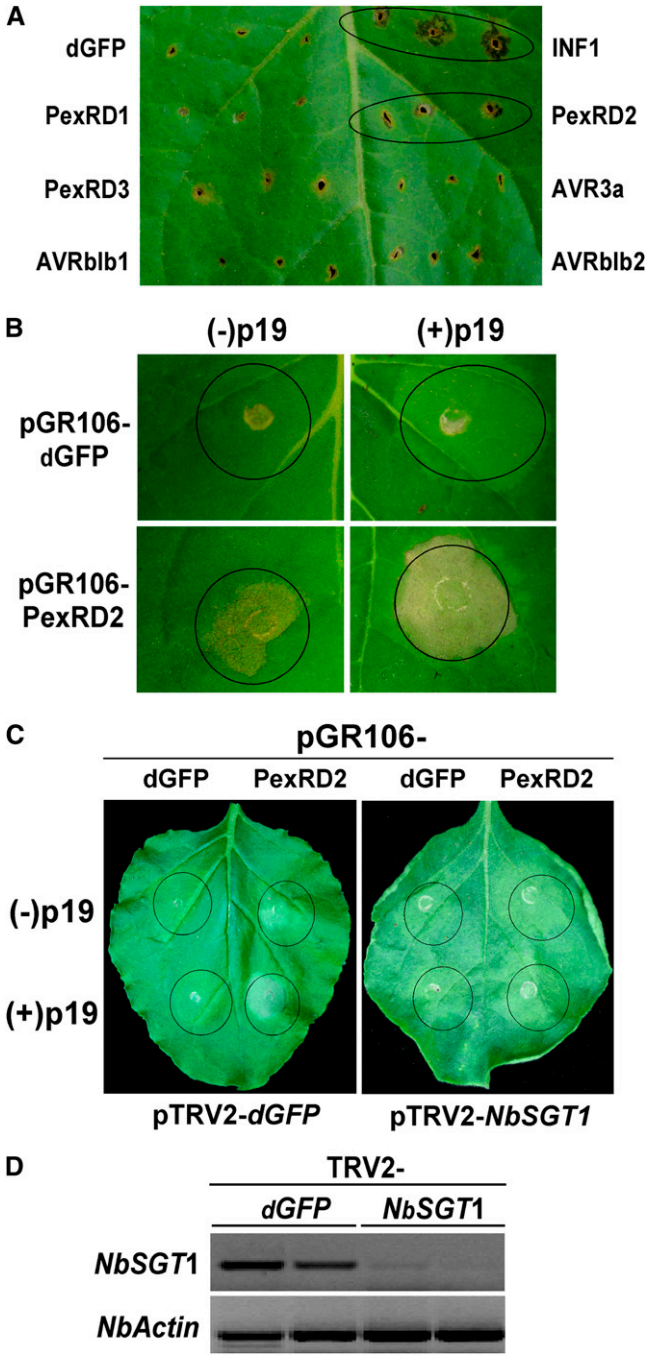

Figure 4. PexRD2 Promotes Cell Death in *N. benthamiana*.

(A) Symptoms observed in *N. benthamiana* after wound inoculation with *A. tumefaciens* carrying pGR106 vector derivatives expressing a subset of the 62 RXLR effectors of *P. infestans*. The negative and positive controls were *A. tumefaciens* strains carrying pGR106-ΔGFP (dGFP) and pGR106-INF1, respectively. Note the small ring of dead cells triggered by the pGR106-PexRD2 strain relative to the more expanded cell death triggered by pGR106-INF1. All strains were inoculated in triplicate. The photo was taken 12 DAI.

(B) The PexRD2-associated cell death is enhanced in the presence of gene silencing suppressor p19. *A. tumefaciens* carrying pGR106-PexRD2 was mixed with (+) p19 or without (−) an *A. tumefaciens* p19 strain and infiltrated into *N. benthamiana* leaves. The experiment was repeated three times with similar results. After 6 d, the PexRD2-associated cell death symptoms were observed in both cases but were enhanced in the presence of p19. All strains were inoculated in triplicate.

(C) SGT1 is required for the cell death response induced by PexRD2. Leaves of *N. benthamiana* vector control (TRV2-dGFP) and SGT1-silenced (TRV2-NbSGT1) plants were challenged by agroinfiltration of *A. tumefaciens* carrying pGR106-ΔGFP (dGFP, negative control) or pGR106-PexRD2. Control-silenced plants showed symptoms of the cell death induced by the PexRD2 starting at 3 to 5 DAI, and this response was enhanced in the presence of gene silencing suppressor p19 (left panel). In the TRV2-NbSGT1 plants, the PexRD2-associated cell death was suppressed (right panel).

(D) RT-PCR analysis of *SGT1* expression in control (TRV2-dGFP) and *SGT1*-silenced (TRV2-NbSGT1) *N. benthamiana*. Total RNA was extracted from the silenced plants and subjected to RT-PCR analysis with *SGT1* primers to detect *SGT1* transcripts. The *Actin* gene was used to confirm equal total RNA amounts among samples. Similar results were obtained at least two times independent experiments.

responses were monitored up to 14 DAI. The screens revealed that two PexRD6/IpiO clones triggered HR-like lesions on *Rpi-blb1* expressing leaves, and 10 clones of the closely related PexRD39 and PexRD40 clones triggered HR on *Rpi-blb2* leaves (Figure 5A; see Supplemental Data Set 1 online).

To confirm these results using a different assay, we performed coagroinfiltration of the two PexRD6/IpiO and two of the PexRD39/40 *A. tumefaciens* pGR106 strains with the two *R* gene strains in *N. benthamiana*. The HR reactions observed in the wound inoculation screen were confirmed (Figures 5B to 5D). In the *Rpi-blb1* coinfiltrations, the HR was observed with the two PexRD6/IpiO clones starting at 4 DAI, and for *Rpi-blb2*, the HR was observed with both PexRD39 and PexRD40 constructs starting at 3 DAI (Figures 5B to 5D). Altogether, these experiments indicate that the identified clones are specifically recognized by the cognate *R* genes. We suggest that PexRD6/IpiO is *Avrblb1* and PexRD39/40 is *Avrblb2*.

The *PexRD6/ipiO* gene was independently identified as *Avrblb1* by Vleeshouwers et al. (2008) using a functional screen on wild *Solanum* plants carrying the *Rpi-blb1* gene. In both studies, $PexRD6_{41\text{-}3}$ (named IpiO1-K143N by Vleeshouwers et al., 2008) and $PexRD6_{41\text{-}10}$ (IpiO2) caused the HR on *Rpi-blb1*-expressing leaves, whereas homolog $PexRD6_{39\text{-}6}$ (IpiO4) failed to trigger cell death (see Supplemental Data Set 1 online).

The *PexRD39* and *PexRD40* genes are close homologs with open reading frames of 303 bp, corresponding to predicted translated products of 100 amino acids. The two predicted proteins differ only in 9 out of 100 amino acids, seven of which are in the mature proteins. Primers based on these two genes amplified overlapping sets of amplicons corresponding to 13 different sequences (see Supplemental Data Set 1 online). Of these, 10 different clones induced the HR on *Rpi-blb2*-expressing leaves in both wounding and agroinfiltration assays, whereas $PexRD39_{89\text{-}2}$, $PexRD39_{89\text{-}7}$, and $PexRD39_{159\text{-}6}$ did not (see Supplemental Data Set 1 online).

PexRD39 and PexRD40 are also similar to other RXLR effectors, namely, PexRD41, PexRD45, and PexRD46 (BLASTP E values < 1e-05), resulting in a superfamily of 21 proteins (see

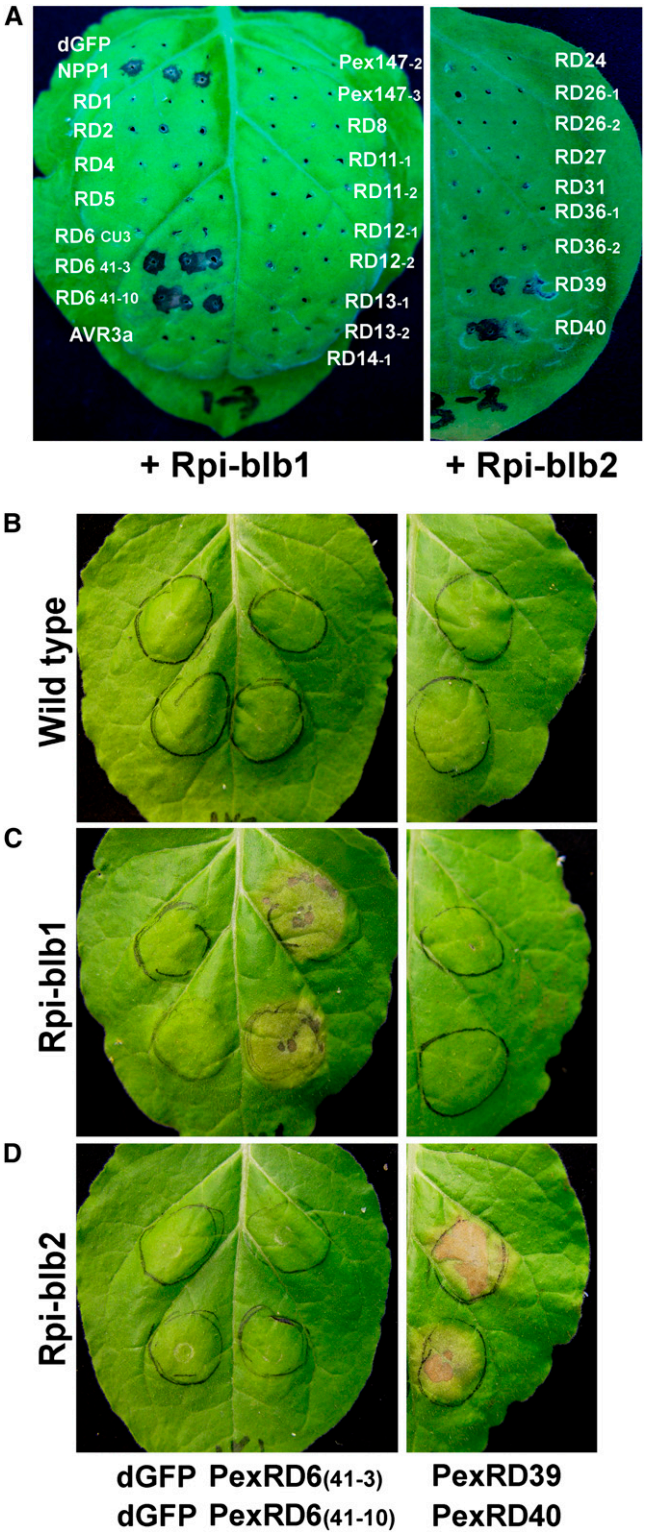

Figure 5. Functional Identification of *Avrblb1* and *Avrblb2*.

(A) Wound inoculation screening of the pGR106-PexRD library on *N. benthamiana* leaves expressing the *S. bulbocastanum R* genes *Rpi-blb1* (left panel) and *Rpi-blb2* (right panel). The two HR-inducing PexRD6/IpiO clones (PexRD6$_{41\text{-}3}$/IpiO1-K143N and PexRD6$_{41\text{-}10}$/IpiO2) and two of the positive PexRD39 and PexRD40 clones (PexRD39$_{169\text{-}6}$ and PexRD40$_{170\text{-}1}$) are shown. Additional PexRD clones that yielded negative responses are also shown. All tested clones are labeled RD# for the corresponding PexRD clone number. The negative and positive controls were *A. tumefaciens* strains carrying pGR106-ΔGFP (dGFP) and pGR106-PiNPP1 (NPP1), respectively.

(B) to **(D)** Confirmation of *Avrblb* cloning using agroinfiltration. Agroinfiltration of the positive *A. tumefaciens* pGR106 strains carrying *Avrblb1* (PexRD6$_{41\text{-}3}$/IpiO1-K143N and PexRD6$_{41\text{-}10}$/IpiO2, top and bottom right panels, respectively) and *Avrblb2* (PexRD39 and PexRD40, top and bottom panels, respectively) was performed in *N. benthamiana* corresponding to control plants **(B)** or leaves expressing *Rpi-blb1* **(C)** or *Rpi-blb2* **(D)**. *A. tumefaciens* strain carrying pGR106-ΔGFP (dGFP) was used as a negative control (top and bottom left panels of leaves). Coinfiltration was performed with *A. tumefaciens* solutions mixed in 1:2 ratio (*Avr:R* gene). Hypersensitive cell death was observed starting at 4 DAI, and the photograph was taken at 7 DAI. The experiment was repeated three times with similar results.

Supplemental Table 3 online). However, none of these additional homologs induced the HR on *Rpi-blb2*-expressing leaves.

The *Avrblb2* Family Is Highly Variable and under Diversifying Selection in *P. infestans*

We elected to study the *Avrblb2* family in more detail because the forthcoming release of potato cultivars carrying *Rpi-blb2* would benefit from a better understanding of the targeted effector. To mine further sequence polymorphisms of *Avrblb2* in *P. infestans*, we used the strategy that we previously applied for the small Cys-rich protein SCR74 (Liu et al., 2005). We performed PCR amplifications with genomic DNA from six diverse *P. infestans* isolates, 88069, 90128, IPO-0, IPO-428, IPO-566, and US980008 (Table 2; see Supplemental Table 2 online). Direct sequencing of amplicons obtained from genomic DNA of the six isolates resulted in mixed sequences, indicating that the primers amplified multiple alleles or paralogs of *Avrblb2*. Therefore, we cloned the amplicons and generated high-quality sequences (phred Q>20, phred software; CodonCode) of the inserts of 85 different clones. In addition, we included seven *Avrblb2* paralogous sequences from the genome sequence of strain *P. infestans* T30-4 (Haas et al., 2009).

A total of 24 different nucleotide sequences, encoding 19 predicted amino acid sequences, could be identified for *Avrblb2* (Figure 6A, Table 2; see Supplemental Data Set 2 online). Polymorphisms were detected in 24 of the 279 examined nucleotides. None of the *Avrblb2* sequences contained premature stop codons or frameshift mutations. Multiple alignments of the 24 predicted AVRblb2 amino acid sequences revealed a highly polymorphic family (Figure 6A). A total of 14 polymorphic amino acid sites were identified, 10 of which localize to the C-terminal domain (after the RSLR motif).

To determine the selection pressures underlying sequence diversification in the AVRblb2 family, we calculated the rates of nonsynonymous (d_N) and synonymous (d_S) mutations across the 24 sequences. We found that d_N was greater than d_S ($\omega = d_N/d_S > 1$) in 121 of 276 pairwise comparisons (see Supplemental Figure 3 and Supplemental Data Set 3 online). In the C-terminal (after RSLR)

Table 2. Distribution of *Avrblb2* Sequences among *P. infestans* Isolates

Homolog ID	Amino Acid at Position 69	*P. infestans* Isolates						
		T30-4[a]	88069[b]	90128[b]	IPO-0[b]	US980008[b]	IPO-428[b]	IPO-566[b]
D5	Ala	PITG_04090	CV89	NF82		NF18	NF42	NF45
A1	Ala	PITG_20300			NF9		NF32	NF48
I6	Ala		NF71					
K3	Ala		NF61					
J7	Ala				NF12			
F2	Ala					NF17		
G8	Ala					NF22		
E4	Ala						NF44	
B1	Ala							NF58
C1	Ala							NF49
H9	Ala							NF47
O13	Ile	PITG_04086	NF65	NF80		NF16	NF38	NF56
S16	Ile	PITG_18683						
P13	Ile				NF4			
R14	Ile						NF43	
Q13	Ile							NF51
T15	Ile							NF50
L17	Val	PexRD40b	NF66		NF6			
N19	Val		NF67					
M18	Val				NF13			
U10	Phe	PITG_20303	NF62		NF7	NF23		
V11	Phe	PITG_20301	NF63					
W12	Phe				NF2			
X12	Phe				NF11			

[a]The descriptors in this column correspond to the gene ID of the *Avrblb2* paralogs present in the reference strain T30-4 (Haas et al., 2009).
[b]The descriptors in these columns correspond to the clone IDs recovered from each of the strains for each one of the 24 *Avrblb2* homologs

protein regions, d_N exceeded d_S in 71 over 276 possible pairwise comparisons (162 bp) (see Supplemental Figure 3 online). These results provide evidence that positive diversifying selection has acted on the AVRblb2 family, particularly on the C-terminal effector domain.

AVRblb2 Residues under Diversifying Selection

To detect the particular amino acid sites under diversifying selection in the AVRblb2 family, we applied the maximum likelihood (ML) method implemented in the PAML 4.2a software package (Nielsen and Yang, 1998; Yang et al., 2000; Yang, 2007). The discrete model M3 with three site classes revealed that ~12% of the amino acid sites were under strong positive selection with ω_2 = 12.32. The likelihood ratio test (LRT) for comparing M3 with M0 is $2\Delta L = 2 \times[-607.52 - (-630.39)] = 45.74$, which is greater than the χ^2 critical value (13.28 at the 1% significance level, with degrees of freedom = 4) (Table 3). This indicates that the discrete model M3 fits the data significantly better than the neutral model M0, which does not allow for the presence of diversifying selection sites with $\omega > 1$. We then used the empirical Bayes theorem to identify eight amino acid sites (40V, 42P, 47I, 69A, 70Q, 84G, 88E, and 95A) implicated as being under diversifying selection with >95% confidence under the discrete model M3 (Table 3).

We also performed the LRT between the null model M7 (β-distribution) and the alternative model M8 (β+ω distribution). The model M8 showed that ~87% of sites had ω from a U-shaped β-distribution, and ~13% of sites were under strong diversifying selection with ω = 12.3. The difference between model M7 and model M8 was statistically significant, as indicated by the LRT: $2\Delta L = 2 \times[-607.52 - (-622.81)] = 30.58$, which is greater than the χ^2 critical value (9.21 at 1% significance level, with degrees of freedom = 2) (Table 3). Thus, model M8 fitted the data significantly better than model M7. Under model M8, using the empirical Bayes theorem, we identified the same sites under positive selection as the ones identified under model M3, except for the site 40V (Table 3). We plotted the positions of the seven sites under diversifying selection in AVRblb2 (Figure 6B). Interestingly, all seven amino acid sites were located in the mature AVRblb2 protein, with six residues located after the RXLR motif. Again, this independently supports the finding that sites under diversifying selection occur more frequently in the C-terminal region of AVRblb2.

We also proceeded to analyze paralogous sequences following the strategy of Win et al. (2007). Using the same ML methods described above, we analyzed a subset of four paralog sequences of *P. infestans* T30-4 and, remarkably, identified only a single position, amino acid 69, under positive selection (Figure 6C). This indicates that residue 69 can be detected as a positively selected amino acid even using less sensitive analyses and a smaller set of sequences.

AVRblb2 Does Not Require the RXLR Motif for Perception by Rpi-blb2

RXLR effectors are modular proteins with the effector activity carried by the C-terminal domain that follows the RXLR region

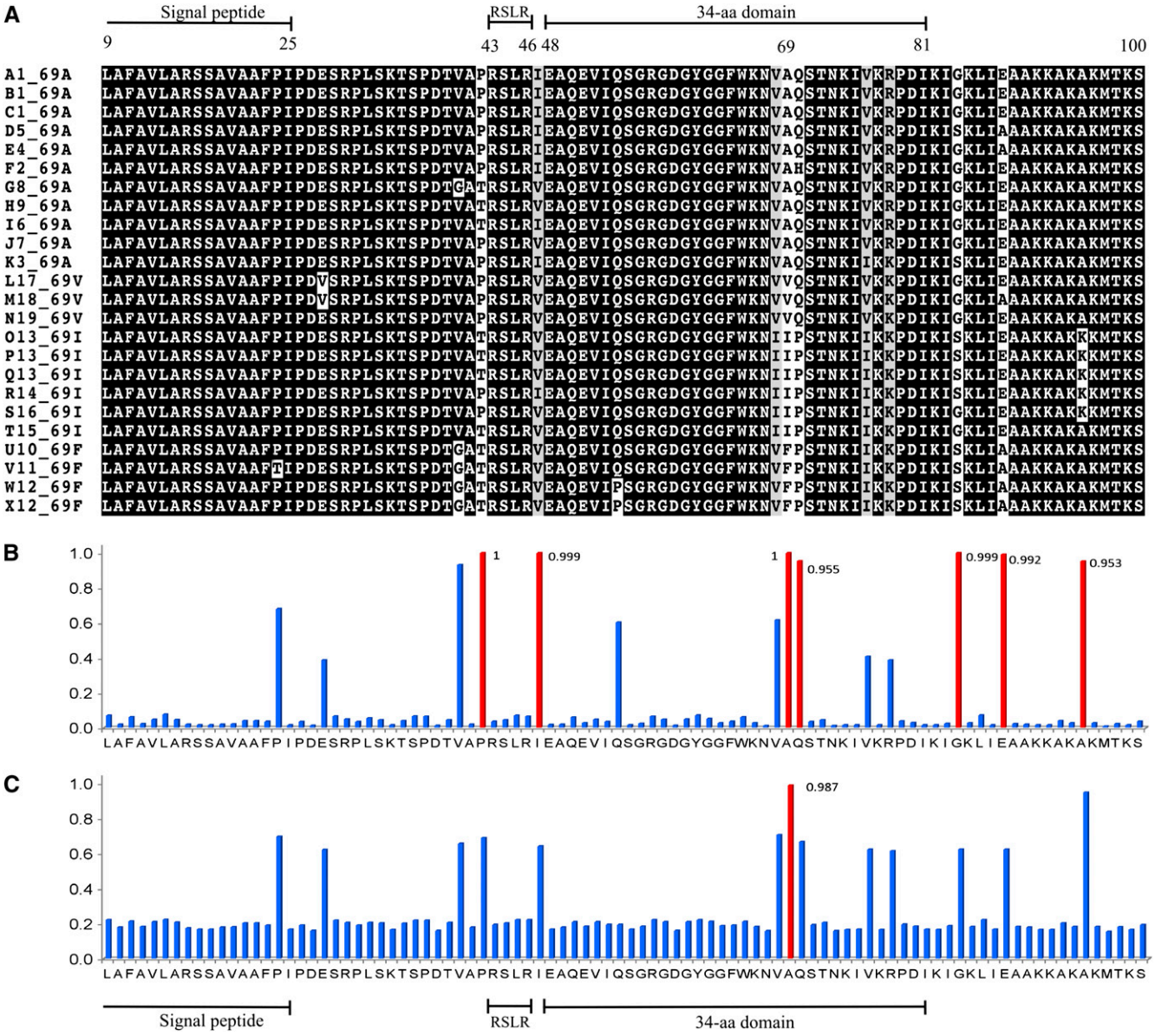

Figure 6. The AVRblb2 Family Is Highly Polymorphic and under Diversifying Selection in *P. infestans*.

(A) Multiple sequence alignment of 24 AVRblb2 amino acid sequences from *P. infestans*. Single-letter amino acid codes were used. Residue numbers are denoted above the sequences. The predicted signal peptide, RSLR motif, and 34–amino acid functional domains are indicated above the alignment.
(B) Posterior probabilities along the AVRblb2 protein sequence for site classes estimated under the discrete model M8 in the PAML software. The analysis was based on the 24 identified AVRblb2 sequences described in Figure 6A. Amino acid sites 42P, 47I, 69A, 70Q, 84G, 88E, and 95A marked in red have high posterior probabilities ($P > 0.95$ and $\omega > 8.9$) and are potentially under positive selection.
(C) Posterior probabilities along the AVRblb2 protein sequence obtained with a subset of four paralogous sequences from *P. infestans* T30-4 strain. In this analysis, only residue 69A ($\omega = 69.434$) is under positive selection. The position of the signal peptide, RSLR motif, and the 34–amino acid domain are indicated below the graphs.

(Bos et al., 2006; Kamoun, 2006, 2007). The RXLR motif is not required for avirulence activity when the protein is directly expressed inside plant cells (Bos et al., 2006; Allen et al., 2008). However, Dou et al. (2008a) showed that the RXLR motif of *P. sojae* Avr1b is required for cell death induction when a full-length construct with the signal peptide is expressed in plant cells, presumably to enable reentry of the protein following secretion. We cloned a full-length *Avrblb2* (*PexRD40*$_{170\text{-}7}$), with its native signal peptide, in the binary PVX vector and found by agroinfiltration that it triggers Rpi-blb2–dependent HR in *N. benthamiana* (Figure 7). To test whether the RSLR motif is required for cell death induction by the full-length AVRblb2, we

Table 3. Likelihood Ratio Test Results for *Avrblb2*

Model	Estimate Parameters	InL[a]	Sites under Selection[b]	Model Comparison	2ΔL[c]	χ^2 Critical Value	Degree of Freedom
Full set							
M0: one ratio		−630.39	Not allowed	M0 vs. M3	45.74	13.28	4
M3: discrete	P_0 = 0.82144 P_1 = 0.05225 P_2 = 0.12631 ω_0 = 0.21145 ω_1 = 0.21145 ω_2 = 12.31659	−607.52	40V **42P 47**I **69A** 70Q **84G 88E** 95A				
M7: β	P = 0.00500 q = 0.00835	−622.81	Not allowed	M7 vs. M8	30.58	9.21	2
M8: β + w	P_0 = 0.87372 P = 29.63451 q = 99.000 P_1 = 0.12628 ω = 12.31969	−607.52	**42P 47**I **69A** 70Q **84G 88E** 95A				
Paralog set							
M0: one ratio		−484.08	Not allowed				
M3: discrete	P_0 = 0.00012 P_1 = 0.97263 P_2 = 0.02725 ω_0 = 2.15645 ω_1 = 2.15649 ω_2 =143.0264	−479.95	**69A**	M0 vs. M3	8.26	13.28	4
M7: β	P = 2.01635 q = 0.00500	−484.63	Not allowed				
M8: β + w	P_0 = 0.97494 P = 4.12227 q = 0.00500 P_1 = 0.02506 ω = 69.43383	−480.38	**69A**	M7 vs. M8	8.50	9.21	2

[a]InL, log likelihood value.
[b]Amino acid sites inferred to be under positive selection with a probability >99% are in bold and >95% are underlined.
[c]Likelihood ratio test: $2\Delta L = 2(\ln L_{\text{alternative hypothesis}} - \ln L_{\text{null hypothesis}})$.

mutated this sequence into ASAA. Agroinfiltration of the mutated *Avrblb2* with *Rpi-blb2* in *N. benthamiana* resulted in a confluent HR similar to the response triggered by the wild-type *Avrblb2* (Figure 7). To account for the possibility that the native AVRblb2 signal peptide is not fully effective in plants and to avoid potential problems due to the PVX expression system, we made new constructs in the *A. tumefaciens* binary vector pCB302-3. The two constructs (RSLR and ASAA mutants), consisting of a fusion between the signal peptide of the tomato Ser protease P69B (Tian et al., 2004) and the mature protein of AVRblb2, triggered Rpi-blb2–mediated HR in *N. benthamiana* (see Supplemental Table 6 online). These data are consistent with the results obtained by Bos et al. (2006) with AVR3a and show that the RXLR motif of AVRblb2 is not required for recognition by Rpi-blb2. However, these experiments remain inconclusive with respect to the potential contribution of the RXLR motif to translocation of the protein inside plant cells in the absence of the pathogen and stand in contrast with the results obtained by Dou et al. (2008a) with Avr1b in soybean (*Glycine max*).

Deletion Analysis of AVRblb2 Identifies a 34–Amino Acid Region Sufficient for Induction of Rpi-blb2–Mediated Cell Death

To delineate the functional domain of AVRblb2, we made a series of deletion constructs and assayed them in *N. benthamiana* (Figure 7). Results obtained with our original pGR106-PexRD constructs indicate that the AVRblb2 homologs do not require a signal peptide sequence to trigger Rpi-blb2–mediated HR (Figure 5) and that the recognition event occurs inside the plant cytoplasm similar to the AVR3a and R3a interaction (Armstrong et al., 2005; Bos et al., 2006). We assayed five N-terminal and C-terminal deletion mutants for activation of Rpi-blb2 cell death by agroinfiltration in *N. benthamiana*. These experiments indicated that a 34–amino acid C-terminal region of AVRblb2 (EAQEVIQSGRGDGYGGFWKNVVQSTNKIVKKPDI) is sufficient for triggering Rpi-blb2–mediated cell death (Figure 7). This 34–amino acid C-terminal region of AVRblb2 excludes the RXLR leader sequence but, interestingly, includes the one polymorphic amino acid at position 69(V) that was identified as positively selected in the ML method (Figure 6).

The Positively Selected Amino Acid 69 of AVRblb2 Is Critical for Activation of Rpi-blb2 Hypersensitivity

The positively selected residue 69 is the only polymorphic residue within the 34–amino acid region that correlates with the HR-inducing activity on Rpi-blb2–expressing leaves. The 10 AVRblb2 homologs that are recognized by Rpi-blb2 have Val-69, Ala-69, or Ile-69, whereas the three that are not recognized have Phe-69. To further evaluate the impact of residue 69 on AVRblb2 activity, we mutated this residue in $PexRD40_{170\text{-}7}$ (referred to as PexRD40 from here on), from Val to Ala, Ile, or Phe and constructed a fusion between the FLAG epitope tag and the mature portion of PexRD40. The corresponding pGR106-FLAG-PexRD40 constructs were used in agroinfiltrations of *N. benthamiana* to express the mature PexRD40 proteins (amino acids 23 to 100) in combination with Rpi-blb2 (Figure 8). In contrast with PexRD40, $PexRD40^{V69A}$, and $PexRD40^{V69I}$, the $PexRD40^{V69F}$ mutant consistently failed to induce Rpi-blb2–mediated hypersensitivity in side-by-side infiltrations (Figures 8B to 8D). Protein gel blot hybridizations of extracts from infiltrated

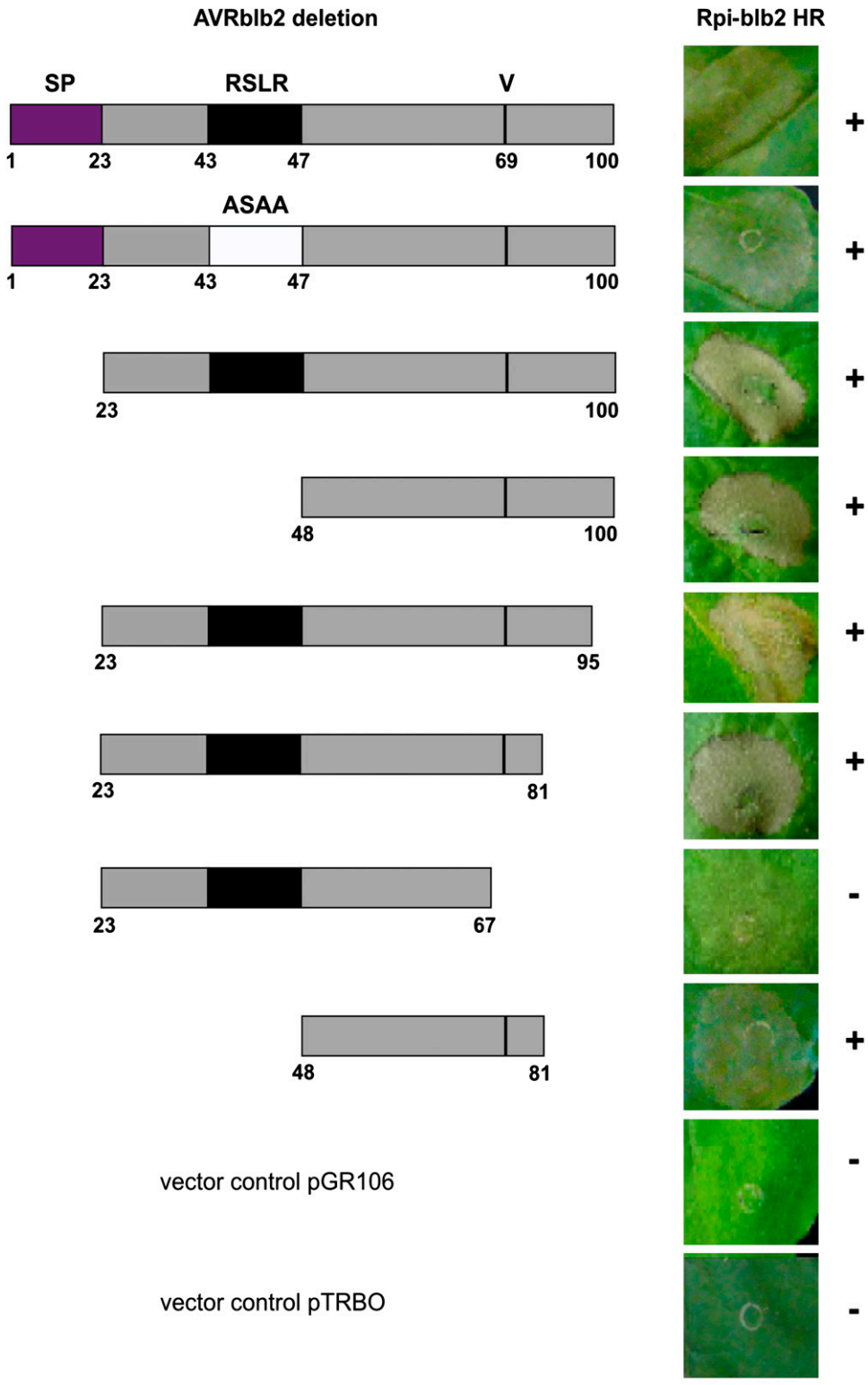

Figure 7. Deletion Analysis of AVRblb2 Reveals a 34–Amino Acid Region Sufficient for Induction of Rpi-blb2–Mediated Cell Death.

RXLR and deletion mutants of PexRD40$_{170\text{-}7}$ were coexpressed with Rpi-blb2 by agroinfiltration in *N. benthamiana* to determine the AVRblb2 domains required for induction of the Rpi-blb2–mediated HR. A schematic view of the different mutant and deletion constructs is shown on the left. Symptoms of infiltration sites coexpressing the AVRblb2 construct with Rpi-blb2 are shown on the right. HR cell death index with plus and minus signs indicate the presence and absence of effector activity, respectively. The assays were repeated at least three times with similar results. Photograph of symptoms were taken 5 to 7 DAI. SP, signal peptide.

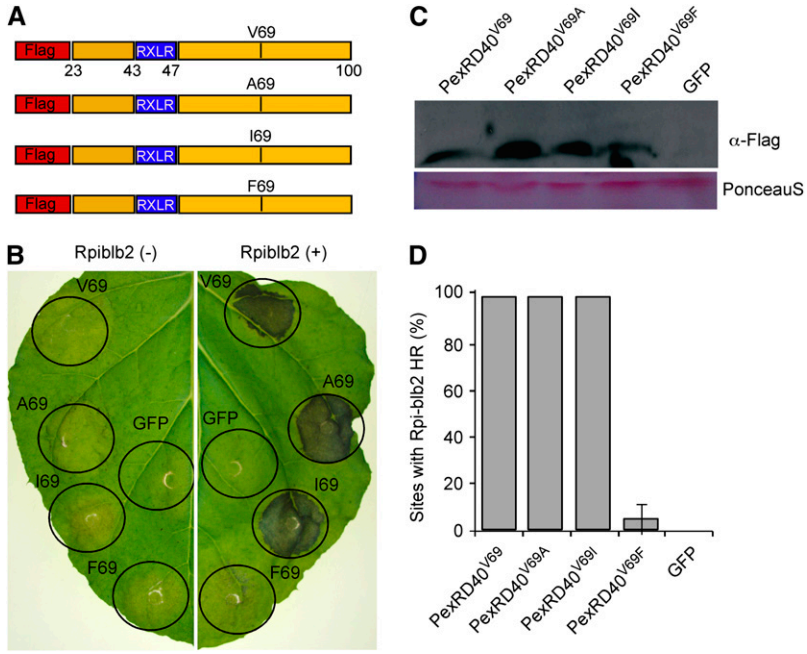

Figure 8. The Positively Selected Amino Acid 69 of AVRblb2 Is Critical for Activation of Rpi-blb2 Hypersensitivity.

(A) Schematic view of pGR106-PexRD40$_{170-7}$ (AVRblb2) site-directed mutant constructs. FLAG refers to the FLAG epitope tag. V (Val), A (Ala); I (Ile), and F (Phe) refer to the amino acids at position 69 with the top construct (V69) corresponding to PexRD40$_{170-7}$. The numbers refer to the amino acid positions based on the full-length protein.

(B) Symptoms observed in *N. benthamiana* infiltration sites coexpressing the PexRD40$_{170-7}$ constructs with (+) or without (−) *Rpi-blb2*. Photographs were taken 6 DAI. *A. tumefaciens* solutions were mixed in a 1:1 ratio before infiltration into *N. benthamiana* leaves. V69, A69, I69, and F69 refer to the constructs described in **(A)**. The negative control was *A. tumefaciens* strains carrying pGR106-ΔGFP (GFP).

(C) In planta accumulation of PexRD40 proteins. A FLAG immunoblot was performed on total protein extracts of leaves of *N. benthamiana* following agroinfiltration with the constructs described in **(A)**. An ~10-kDa protein band representing recombinant PexRD40 was detected in total extracts of plant tissues expressing all PexRD40 constructs but not the ΔGFP negative control. Equal loading was checked by PonceauS staining.

(D) Percentages of infiltration sites with Rpi-blb2–mediated hypersensitive cell death based on two independent experiments scored at 4 DAI. Error bars indicate SE.

N. benthamiana leaves with FLAG antisera revealed no differences in intensity between the four FLAG-PexRD40 proteins (Figure 8C). We conclude that the proteins are equally stable in planta and that the difference in Rpi-blb2–mediated HR cannot be attributed to PexRD40^{V69F} protein instability. Taken together, these results along with the phenotypes observed with the 13 AVRblb2 homologs and the delimitation of the avirulence activity to the 34–amino acid region indicate that the positively selected residue 69 is critical for perception by Rpi-blb2.

DISCUSSION

In this study, we employed an effectoromics strategy to perform high-throughput screens for effector activity using a library of 62 candidate RXLR effectors from the potato late blight pathogen *P. infestans*. We were successful in assigning an effector activity to 16 of the assayed 62 proteins, including suppression of cell death, as well as nonspecific and R protein–mediated elicitation of cell death. These results further support the view that functional genomics pipelines can be particularly successful to identify effectors from mined sequence data (Torto et al., 2003; Kamoun, 2006). We increased our success rate by refining the criteria for selecting candidates and focusing only on the RXLR effector class. In addition, we took advantage of the PVX agroinfection method that enables sensitive and high-throughput in planta expression assays by wound inoculation (Takken et al., 2000; Nasir et al., 2005; Takahashi et al., 2007; Vleeshouwers et al., 2008; Bos et al., 2009).

Haas et al. (2009) recently predicted a total of 563 RXLR effector genes, grouped in 149 families, from the genome sequence of *P. infestans* strain T30-4. Our library of 62 clones obtained from 32 primer pairs was generated prior to the completion of the genome sequence and at first glance may appear poorly representative of RXLR effector diversity in *P. infestans*. Nonetheless, we successfully identified two *Avr* genes as well as novel elicitors and suppressors of cell death and assigned activities to 16 of the 62 effectors. How can such a high success rate be obtained with an apparently underrepresentative library? One explanation is that the majority of the selected genes are expressed because they were mined from *P. infestans* EST data sets (Kamoun et al., 1999a; Randall et al., 2005). Indeed, 27

(84%) out of our 32 candidates are induced in planta (see Supplemental Table 4 online), whereas of the total RXLR effectors predicted by Haas et al. (2009) only 129 (23%) of the 563 are induced in potato. These results further confirm the observation that selecting candidate effectors from cDNA sequences can be extremely productive even in the absence of a genome sequence (Torto et al., 2003; Tian et al., 2004; Liu et al., 2005). Nonetheless, in the future, an expanded genome-wide collection covering at least all the expressed effectors will provide an even more useful resource.

Suppression of plant innate immunity has emerged as the primary function of bacterial effectors and is likely to be an important activity of oomycete, fungal, and nematode effectors as well (Block et al., 2008; Hogenhout et al., 2009). Nevertheless, our screen of suppressors of cell death response triggered by the PAMP-like secreted protein INF1 revealed only two new effectors in addition to AVR3a^{KI}. These effectors, PexRD8 and PexRD36$_{45\text{-}1}$, suppressed the HR induced by INF1 at lower levels than AVR3a^{KI} (Figure 3) and therefore may have limited impact on pathogen virulence. In addition, this result reveals a limited degree of redundancy in suppression of INF1-mediated hypersensitivity and that this suppressor activity is not a widespread feature of RXLR effectors. These findings stand in contrast with the recent observation that the majority of the 35 TTSS effectors of *P. syringae* DC3000 suppress the HR induced by the bacterial effector HopA1 (Guo et al., 2009). This indicates a significantly higher degree of redundancy among *P. syringae* TTSS effectors relative to *P. infestans* RXLR effectors. How so many functionally redundant effectors are maintained in a pathogen genome remains a puzzling question.

The promotion of cell death elicited by PexRD2 could reflect the effector activity of this protein. Ectopic expression of numerous bacterial Type III secretion system effectors (Kjemtrup et al., 2000; Cunnac et al., 2009; Gurlebeck et al., 2009) and *P. infestans* Crinklers (Torto et al., 2003; Haas et al., 2009) is known to alter host immunity, resulting in tissue necrosis, browning, and chlorosis. In *Pseudomonas syringae*, 14 TTSS effectors elicit cell death when expressed in *N. benthamiana* or *Nicotiana tabacum* (Cunnac et al., 2009). Additional assays with pGR106-PexRD2 indicated that the observed cell death response is nonspecific and occurs also in the host plant potato as well as 10 additional *Solanum* species (Vleeshouwers et al., 2008).

The biological relevance of nonspecific cell death promotion by effectors remains ambiguous. One possibility is that promotion of cell death could reflect the virulence function of PexRD2, perhaps as a result of excessive activity on an effector target (Cunnac et al., 2009). This possibility is further strengthened by the emerging view that effectors are promiscuous proteins that bind more than one host target (Van der Hoorn and Kamoun, 2008; Hogenhout et al., 2009). Therefore, the cell death elicitation phenotype could have resulted from aberrant activation of host targets other than the operative target (Van der Hoorn and Kamoun, 2008). In addition, the cell death phenotype could be due to the artificially high expression levels of PexRD2, which is inherent to the *A. tumefaciens*–based assay. Alternatively, the effectors could trigger the HR in a typical avirulence fashion. This is supported by our finding that PexRD2-mediated cell death is dependent on the ubiquitin ligase-associated protein SGT1 (Figures 4C and 4D), which is required for nucleotide binding site–leucine-rich repeat (NBS-LRR) protein activity (Austin et al., 2002; Azevedo et al., 2002; Peart et al., 2002). However, in side-by-side assays, PexRD2 triggered a much weaker response than the HR elicited by *P. infestans* AVR proteins or INF1 (Figures 4A and 5A), and the *PexRD2* gene is conserved in *P. infestans* with no evidence of diversifying selection (Table 1). Nonetheless, PexRD2 cell death may have resulted from weak recognition by an *N. benthamiana* NBS-LRR protein. In such a case, the activity of this NBS-LRR protein must be conserved in other plants, such as potato and tomato, possibly through the recognition of a conserved solanaceous protein targeted by PexRD2.

Vleeshouwers et al. (2008) recently identified AVRblb1 by screening an earlier version of the *PexRD* library on late blight resistant *Solanum* genotypes. Here, we independently isolated and confirmed the identity of AVRblb1 as IPIO (PexRD6) using coexpression with *S. bulbocastanum* Rpi-blb1 in *N. benthamiana*. In addition, we discovered candidate AVRblb2 (PexRD39/40), a previously unknown family of effectors that activate a different *S. bulbocastanum* gene, *Rpi-blb2*. These genes trigger *Rpi-blb2*–specific hypersensitivity following heterologous expression in *N. benthamiana*, but independent confirmation of their identity as AVRblb2 will require isogenic *P. infestans* strains with differential virulence.

The finding that some of the *Avrblb1* and *Avrblb2* alleles are not, or are weakly, recognized by their cognate *Rpi-blb* gene suggests that they may have evolved to evade recognition by resistant *Solanum* plants. A degree of coevolution between *P. infestans* and host plants carrying *R* genes with *Rpi-blb1* and *Rpi-blb2* activities is likely. Although *S. bulbocastanum* is distributed outside the known natural range of wild *P. infestans* populations, *Rpi-blb*–like activities were noted in wild *Solanum* spp that are naturally infected by *P. infestans* at its center of diversity in Toluca Valley, Mexico (Vleeshouwers et al., 2008); thus, virulent *Avrblb* alleles may have evolved. With the *Avrblb* genes at hand, we are now in a position to monitor the potential emergence of virulent races that may accompany the agricultural deployment of the *Rpi-blb* genes and rigorously assess the broad-spectrum activities reported for *Rpi-blb1* and *Rpi-blb2* (Helgeson et al., 1998; Song et al., 2003; van der Vossen et al., 2003; Kuhl et al., 2007; Halterman et al., 2008).

Cloning of the *Avrblb* genes has consequences for understanding the basis of broad-spectrum disease resistance mediated by the *Rpi-blb* genes. Until recently, the only *R* genes available to potato breeders have been the *R1* to *R11* genes originating from *S. demissum*. However, the usefulness of these *R* genes proved short-lived because virulent races of *P. infestans* rapidly emerged following the introduction of resistant potato cultivars (Fry, 2008). Two *Avr* genes, *Avr3a* and *Avr4* (also termed *PiAvr4*), perceived by *S. demissum R3a* and *R4*, respectively, have been identified (Armstrong et al., 2005; van Poppel et al., 2008). *Avr4* occurs as a single-copy gene in the *P. infestans* genome, while *Avr3a* is the only expressed gene among a small gene family (Armstrong et al., 2005; Haas et al., 2009; van Poppel et al., 2008). Isolates virulent on R3a potatoes carry the allele *Avr3a^{EM}*, which unlike its counterpart *Avr3a^{KI}*, is not recognized by R3a (Armstrong et al., 2005). *P. infestans* isolates virulent on R4 potatoes carry pseudogenized or deleted loss-of-function

alleles of *Avr4* (van Poppel et al., 2008). *Avrblb1* and *Avrblb2* differ from these genes by occurring as expanded gene families with several paralogs targeted by the cognate *Rpi-blb* gene. Therefore, multiple independent mutations would be required for *P. infestans* to become virulent on *Rpi-blb* potatoes possibly delaying the emergence of virulent races. In addition, the *Avrblb* genes are likely important for *P. infestans* fitness since the pathogen always carries intact coding sequences of these genes. Future functional and population studies, as well as cloning of additional *P. infestans Avr* genes, will help to identify the features of the *Avrblb* genes that make them less likely to overcome rapidly their cognate *R* genes.

AVRblb2 carries a conserved RXLR motif (RSLR) but lacks the dEER sequence that is found in the majority of validated oomycete effectors, confirming that the dEER motif is not absolutely invariant in RXLR effectors (Rehmany et al., 2005; Win et al., 2007). This is surprising because mutations in the dEER motifs of *P. sojae* AVR1b and *P. infestans* AVR3a were shown to abolish avirulence in transgenic strains, suggesting that this motif is required for host translocation (Whisson et al., 2007; Dou et al., 2008a). The RXLR-dEER motifs are known to define a host translocation domain of ~25 to 30 amino acids (Bhattacharjee et al., 2006; Whisson et al., 2007; Dou et al., 2008b; Grouffaud et al., 2008). One possibility is that IEAQEVIQSGR, the sequence immediately following the RSLR motif in AVRblb2, is functionally similar to the dEER sequence.

The C-terminal effector region of AVRblb2 that follows the RSLR sequence is only 54 amino acids making it unlikely that AVRblb2 directly performs an enzymatic activity. Most likely, AVRblb2 carries out its virulence and avirulence activities by binding one or more host proteins. At this stage, we cannot rule out that AVRblb2 directly binds Rpi-blb2, possibly through the 34–amino acid region that is sufficient for activation of hypersensitive cell death. Similar to *H. arabidopsidis* ATR13 (Allen et al., 2004, 2008) and *Melampsora lini* AVRL567 (Dodds et al., 2004, 2006), AVRblb2 displays very high levels of polymorphism (10 polymorphic sites out of 54 in the effector domain) and diversifying selection (up to eight sites under positive selection). How these effectors can be so polymorphic while maintaining their virulence activities remains unclear.

Sequence comparisons of AVRblb2 homologs with differential activities combined with site-directed mutagenesis highlighted residue 69 as critical for recognition by Rpi-blb2. Remarkably, the maximum likelihood method implemented in the codeml program pointed to amino acid 69 as the only positively selected residue when paralogous sequences were used following the strategy of Win et al. (2007). This confirms that positive selection tests on paralogous genes obtained from a single genome sequence can be useful predictors of functionally critical residues (Win et al., 2007).

We observed that the RXLR sequence is not required for cell death induction when a full-length construct containing the native signal peptide is expressed in plant cells (Figure 7) consistent with our previous experiments with AVR3a (Bos et al., 2006). However, these results fail to confirm the findings of Dou et al. (2008a) who showed using a biolistic assay that the RXLR sequence is required for cell death inducing activity when a full-length AVR1b is expressed in soybean cells. We further explored this discrepancy by expressing in *N. benthamiana* several combinations of sequences that add up to five constructs to assess the effect of different parameters on this experiment. The constructs correspond to (1) three different vectors, including viral and nonviral vectors; (2) three different signal peptides, including signal peptides from the tomato proteins PR1a and P69B; and (3) three different RXLR domains, including *P. sojae* AVH1b RXLR domain, which is identical to AVR1b (see Supplemental Table 6 online). In all cases, we failed to detect any effect caused by the RXLR to AXAA mutation and equal levels of cell death induction were noted (see Supplemental Table 6 online). In summary, we view these experiments as inconclusive with regards to the ability of RXLR effectors to enter plant cells in the absence of the pathogen. One possible explanation is that the signal peptides are not fully effective and that mis-targeting of the RXLR effectors from the endoplasmic reticulum into the cytoplasm takes place, resulting in intracellular protein accumulation and activation of cell death.

This study is an initial attempt to address the challenge of assigning biological functions to the enormous number of effector genes unraveled by sequencing the *P. infestans* genome. Here, we further validate the approach of screening effectors by expressing them directly inside plant cells (Torto et al., 2003; Vleeshouwers et al., 2008; Guo et al., 2009; Wroblewski et al., 2009). The diverse activities ascribed here to several RXLR effectors support the view that these proteins form a critical class of host translocated effectors in oomycetes. Detailed analyses of the AVRblb2 family revealed a highly polymorphic and complex family in *P. infestans* and offered insights into the modular structure of this protein. The challenge now is to identify the host targets of effectors like AVRblb2 and understand how these effectors perturb host processes.

METHODS

Microbial Strains, Plants, and Culture Conditions

Escherichia coli DH5α and *Agrobacterium tumefaciens* GV3101, GV2260, and AGL0 (Hellens et al., 2000) were routinely grown in Luria-Bertani (LB) media (Sambrook and Russell, 2001) with appropriate antibiotics at 37 and 28°C, respectively. All bacterial DNA transformations were conducted by electroporation using standard protocols (Sambrook and Russell, 2001). *Phytophthora infestans* strains (see Supplemental Table 2 online) were cultured on rye sucrose agar (Caten and Jinks, 1968) at 18°C. For genomic DNA and RNA extractions, plugs of *P. infestans* mycelium were transferred to modified Plich medium (Kamoun et al., 1993) and grown for 2 weeks before harvesting. *Nicotiana benthamiana* and tomato (*Solanum lycopersicum* cv Ohio 7814) plants were grown and maintained at 22 to 25°C in controlled greenhouse under 16/8-h light-dark photoperiod.

PexRD Gene Selection and Cloning

The *PexRD* genes were mined from a large collection of >80,000 ESTs (Randall et al., 2005). Initially, a set of 50 genes was selected, but this was reduced to 32 genes because 18 genes either failed to fulfill the RXLR effector prediction criteria of Win et al. (2007) or were problematic (poor PCR amplifications, incomplete open reading frames, etc.). Primers corresponding to the 32 candidate RXLR effector genes (see Supplemental Table 1 online) were used in PCR amplification reactions with genomic DNA from 26 *P. infestans* isolates as template (see

Supplemental Table 2 online). None of the examined 32 genes carry introns. The *PexRD* derivatives were amplified by PCR using the oligonucleotide combinations indicated in Supplemental Table 1 online and then cloned into the *Cla*I and *Not*I sites of the *A. tumefaciens* binary PVX vector pGR106 (Lu et al., 2003). The sequences of the pGR106 inserts of the entire collection of *PexRD* clones are shown in Supplemental Data Set 1 online. A DNA fragment corresponding to 34 amino acids of AVRblb2 (residues 48 to 81) was synthesized by GenScript and inserted into the *Pac*I and *Not*I sites of *Tobacco mosaic virus* binary vector pJL-TRBO (Lindbo, 2007) because its small size prevented cloning into pGR106. All other deletion mutants were obtained by PCR amplifications using appropriate primers (see Supplemental Table 7 online) and cloned into pGR106. Site directed mutants of AVRblb2 were generated by overlap extension PCR using high-fidelity *Pfu* polymerase (Stratagene) as described previously (Kamoun et al., 1999b) using the primers described in Supplemental Table 7 online or were synthesized by GenScript. The pGR106-FLAG-AVRblb2 constructs were generated using the oligonucleotides PVX_FLAG-F and PVX_FLAG-R (see Supplemental Table 7 online) and were digested with the *Cla*I and *Not*I restriction enzymes for cloning into the pGR106 vector. As a negative control for the PVX assays, we used the pGR106-ΔGFP construct carrying a truncated and reversed fragment of the *GFP* gene (Bos et al., 2006). All constructs were verified by sequencing.

RT-PCR Analysis

Time courses of *P. infestans* infection of detached tomato leaves were performed using zoospore droplet inoculations as described by Kamoun et al. (1998). Discs of equal sizes surrounding the inoculation droplets were dissected from infected leaves and frozen in liquid nitrogen for immediate use or stored at –80°C for later RNA extraction. Total RNA was extracted from infected tomato leaves using the TRIZOL solution (Invitrogen). First-strand cDNA was synthesized using 2 μg of total RNA, oligo (dT) primer, and M-MLV reverse transcriptase (Invitrogen) according to the manufacturer's instructions. The oligonucleotides used to amplify *PexRD* transcripts are listed in Supplemental Table 1 online. All primer pairs used for RT-PCR amplified PCR products of the expected size from genomic DNA of *P. infestans* 88069 and 90128. All RT-PCR amplifications were confirmed using at least a second independent replicate of the infection time course and by comparison to independently published expression analyses of potato (*Solanum tuberosum*) infections (Whisson et al., 2007; Haas et al., 2009). Controls consisted of the constitutive *ef2α* (Torto et al., 2002) and the in planta–induced *epi1* (Tian et al., 2004).

For RT-PCR analysis in the VIGS experiment, total RNA was extracted from control (dGFP) and SGT1-silenced *N. benthamiana* leaves using the TRIZOL solution. RT-PCR was performed on equal amounts of total RNA using the One-Step RT-PCR kit (Promega). Primers used to amplify *SGT1* annealed outside the VIGS target region and were 5′-TCGCCGTTGACCTGTACACTCAAGC-3′ and 5′-GCAGGTGTTATCTTGCCAAACAACCTAG-3′ (Liu et al., 2002). Primers for the constitutive actin gene were 5′-TGGTCGTACCACCGGTATTGTGTT-3′ and 5′-TCACTTGCCCATCAGGAAGCTCAT-3′.

Plant Assays

Agroinfiltration (*A. tumefaciens* infiltration) and agroinfection (delivery of PVX via *A. tumefaciens*) experiments were performed on 4- to 6-week-old *N. benthamiana* plants using previously described methods (Van der Hoorn et al., 2000; Torto et al., 2003; Huitema et al., 2004). For agroinfiltration assays, recombinant *A. tumefaciens* strains were grown as described elsewhere (Van der Hoorn et al., 2000) except that culturing steps were performed in LB media supplemented with 50 μg/mL of kanamycin (Sambrook and Russell, 2001). The cells were collected by centrifugation (2000*g*, 20 min, 10°C). *A. tumefaciens* strains carrying the respective constructs were mixed in a 2:1 ratio in inducing media (10 mM $MgCl_2$, 10 mM MES, pH 5.6, and 200 μM acetosyringon), and then incubated at room temperature for 3 h before infiltration. *A. tumefaciens* solutions were infiltrated at an OD_{600} of 0.4.

Transient coexpression of *PexRD2* and *p19*, the suppressor of post-transcriptional gene silencing from *Tomato bushy stunt virus* (Voinnet et al., 2003; Lindbo, 2007), was performed by mixing the appropriate *A. tumefaciens* strains in induction buffer at a ratio of 1:1 (final OD_{600} of 0.6). For the cell death suppression assays, *A. tumefaciens* strains expressing the PexRD effectors (pGR106 constructs described earlier) or controls were first infiltrated with a final OD_{600} of 0.3. The infiltration sites were challenged 1 d later with recombinant *A. tumefaciens* carrying p35S-INF1 at a final OD_{600} of 0.3 as previously described (Bos et al., 2006, 2009). For the AVR screens, first, the entire area of *N. benthamiana* leaves was infiltrated with an *A. tumefaciens* strain carrying the appropriate *Rpi-blb* gene (van der Vossen et al., 2003, 2005). One day later, the leaves were challenged by wound inoculation with the *A. tumefaciens* pGR106-PexRD library (see Supplemental Data Set 1 online) along with appropriate positive and negative controls. All clones were inoculated in triplicate, and typically 20 different clones (60 inoculation sites) could be assayed per leaf (Figure 5A).

For VIGS assays, *A. tumefaciens* cultures containing TRV-derived plasmids (TRV1, TRV2-dGFP, and TRV2-NbSGT1; Liu et al., 2002) were transferred into 50 mL of fresh LB media with antibiotics (50 mg/L kanamycin and 25 mg/L rifampicin) and grown at 28°C to an A_{600} of 0.8. The culture was centrifuged, resuspended in 10 mM $MgCl_2$, 10 mM MES, and 150 μM acetosyringone, and kept at room temperature for 3 h before infiltration. Separate cultures containing *A. tumefaciens* strain GV2260 (with TRV2-dGFP and TRV2-NbSGT1 constructs) were mixed in a 1:1 ratio (OD_{600} = 0.3) with GV2260 (TRV1) and infiltrated into the expanded leaves of 4-week-old *N. benthamiana*. The inoculated plants were placed in a growth room at 24°C, 60% relative humidity, and in a 16/8-h light-dark cycle. A set of 10 plants was used; five plants were inoculated with the negative control TRV2-dGFP vector construct, and five plants were inoculated with the TRV2-NbSGT1 construct. At day 21 after inoculation, transient coexpression of *PexRD2* and *p19* (both in GV3101) was performed by mixing the appropriate *A. tumefaciens* cultures in induction buffer at a ratio of 1:1 (final OD_{600} of 0.6). Silenced leaves were sampled for RNA extraction for RT-PCR analysis as described above.

Yeast Signal Sequence Trap System

We used the yeast signal trap system based on vector pSUC2T7M13ORI (pSUC2), which carries a truncated invertase gene, *SUC2*, lacking both the initiation Met and signal peptide (Jacobs et al., 1997). DNA fragments coding for the signal peptides and the following two amino acids of PexRD6/IpiO, PexRD8, PexRD39, and PexRD40 were synthesized by GenScript and introduced into pSUC2 using *Eco*RI and *Xho*I restriction sites to create in-frame fusions to the invertase (see Supplemental Table 5 online). Next, the invertase negative yeast strain YTK12 (Jacobs et al., 1997) was transformed with 20 ng of each one of the pSUC2-derived plasmids individually using the lithium acetate method (Gietz et al., 1995). After transformation, yeast was plated on CMD-W (minus Trp) plates (0.67% yeast N base without amino acids, 0.075% W dropout supplement, 2% sucrose, 0.1% glucose, and 2% agar). Transformed colonies were transferred to fresh CMD-W plates and incubated at 30°C, and transformation status was confirmed by PCR with vector-specific primers. To assay for invertase secretion, colonies were replica plated on YPRAA plates (1% yeast extract, 2% peptone, 2% raffinose, and 2 μg/mL antimicyn A) containing raffinose and lacking glucose. Also, invertase enzymatic activity was detected by the reduction of TTC to insoluble red colored triphenylformazan as follows. Five milliliters of sucrose media were inoculated with the yeast transformants and incubated for 24 h at 30°C. Then, the pellet was collected, washed, and resuspended in

distilled sterile water, and an aliquot was incubated at 35°C for 35 min with 0.1% of the colorless dye TTC. Colorimetric change was checked after 5 min incubation at room temperature (Figure 2).

Avrblb2 Polymorphism Analysis

We used the strategy of Liu et al. (2005) to amplify *Avrblb2* from six *P. infestans* isolates using high-fidelity *Pfu* polymerase (Stratagene). Amplicons were cloned into the pGEM-T vector (Promega). Sequence analyses were performed as detailed below. The reliability of each of the 24 single nucleotide polymorphisms (SNPs) identified was confirmed as follows. First, 18 out of 24 SNPs were recovered from more than one strain and therefore from independent PCR amplifications. All SNPs, including the remaining six SNPs that were only detected in one strain, were confirmed by analyzing chromatograms obtained by sequencing amplicons from two independent PCR amplifications. In addition, all SNPs that were detected in strain T30-4 were also independently double checked with the *P. infestans* genome sequence (Haas et al., 2009).

Sequence Analysis

Similarity searches and the majority of the other bioinformatics analyses were performed locally on Mac OSX workstations using standard bioinformatics programs such as BLAST 2.2.11 (Altschul et al., 1997), HMMer (http://hmmer.janelia.org/; Eddy, 1998), ClustalW (http://www.clustal.org/; Chenna et al., 2003), Sequencher 4.8 (Gene Codes), and SignalP 2.0 (http://www.cbs.dtu.dk/services/SignalP-2.0/; Nielsen et al., 1997), as well as customized Perl scripts (Win et al., 2006, 2007). Multiple alignments were conducted using MUSCLE (Edgar, 2004). For the *Avrblb2* polymorphism analysis, only sequences with phred Q values higher than 20 were retained. Sequences were aligned, and ambiguous calls were checked against chromatograms using Sequencher 4.1 (Gene Codes).

Positive Selection Analyses

For the positive selection analyses, we closely followed the procedures previously described by Liu et al. (2005) and Win et al. (2007). We calculated the rates of nonsynonymous nucleotide substitutions per nonsynonymous site (d_N) and the rates of synonymous nucleotide substitutions per synonymous site (d_S) across pairwise comparisons using the approximate methods of Yang and Nielsen (2000) and Nei and Gojobori (1986) implemented in the YN00 program in the PAML 4.2a software package (Yang, 2007). We also applied the ML method using the computer program codeml from the PAML 4.2a package (Yang, 2007). We used the codon substitution models M0, M3, M7, and M8. Models M3 and M8 allow for heterogeneous selection pressures across codon sites, while their respective null models M0 and M7 only allows ratio classes with $\omega < 1$. Statistical significance was tested by comparing the null models M0 and M7 with their respective alternative models M3 and M8 using an LRT. Twice the difference in log likelihood ratio was compared with a χ^2 distribution with two degrees of freedom. The LRT assesses whether the M3 and M8 alternative models fit the data better than the null M0 and M7 models and is known to be conservative in simulation tests (Anisimova et al., 2001; Thomas, 2006). Positively selected sites were identified using the Bayes Empirical Bayes analysis implemented in codeml (Yang et al., 2005).

Immunoblot Analyses

Leaf tissue was harvested 5 DAI, and proteins were extracted as described by Moffett et al. (2002). The protein expression levels of recombinant PexRD40, PexRD40^{V69A}, PexRD40^{V69I}, and PexRD40^{V69F} were determined by SDS-PAGE and protein gel blotting as described by Tian et al. (2004). Monoclonal FLAG M2 antibody (Sigma-Aldrich) was used as a primary antibody, and anti-mouse antibody conjugated to horseradish peroxidase (Sigma-Aldrich) was used as a secondary antibody at 1:3000 and 1:20,000 dilutions, respectively. Blots were developed using the Pierce Horseradish Peroxidase detection kit (Thermo Scientific) and exposed for 10 min on Amersham Hyperfilm ECL (GE Healthcare). Blots were stained with Ponceau S to estimate protein loading.

Accession Numbers

Sequence data from this article can be found in GenBank under the following accession numbers: AATU01000000 (*P. infestans* T30-4 genome sequence), GQ869413-GQ869474 (inserts of 62 PexRD clones; see Supplemental Data Set 1 online), and GQ869389-GQ869412 (*Avrblb2* sequences; see Supplemental Data Set 2 online).

Supplemental Data

The following materials are available in the online version of this article.

Supplemental Figure 1. RT-PCR Expression Analysis of *PexRD* Genes.

Supplemental Figure 2. Besides AVR3a^{KI}, PexRD8 and PexRD36-1 Suppress the Hypersensitive Cell Death Induced by INF1.

Supplemental Figure 3. Pairwise Comparison of Nucleotide Substitution Rates in 24 AVRblb2 Sequences from *Phytophthora infestans*.

Supplemental Table 1. Primer Sets Used for Allele Mining, Cloning, and RT-PCR of the *PexRD* Genes.

Supplemental Table 2. *Phytophthora infestans* Isolates Used in This Study.

Supplemental Table 3. PexRD Families.

Supplemental Table 4. *PexRD* Genes Shown to Be Induced in Potato by Whisson et al. (2007) and Haas et al. (2009).

Supplemental Table 5. *PexRD* Signal Peptide Sequences Fused to Invertase in the pSUC2 Vector.

Supplemental Table 6. Summary of Experiments Evaluating the Effect of the RXLR Motif on Cell Death Induction by Constructs Carrying a Signal Peptide.

Supplemental Table 7. Primer Sets Used for Cloning of *Avrblb2* Deletion Constructs and Their Corresponding Plasmids.

Supplemental Data Set 1. Infection-Ready Collection of 62 Nonredundant *Phytophthora infestans* RXLR Effectors.

Supplemental Data Set 2. *Avrblb2* Sequences Identified in *Phytophthora infestans*.

Supplemental Data Set 3. Pairwise Comparison of the Ratios ($\omega = d_N/d_S$) of Nonsynonymous (d_N) to Synonymous Nucleotide Substitution (d_S) Rates and d_N and d_S Values among 24 *Avrblb2* Sequences.

ACKNOWLEDGMENTS

We thank I. Malcuit and D. Baulcombe for providing pGR106, John Lindbo for pJL3-p19 and pJL-TRBO, and Kerilynn Jagger, Diane Kinney, and Oluwaseun Layomi Fakunmoju for technical assistance. We are grateful to the Effector Study Group at the Plant Pathology Department, Kansas State University (Vanesa Segovia, Martha Giraldo, Mauricio Montero, Ismael Badillo, and Chang Hyun Khang) for reviewing a draft of the manuscript. This research was supported by National Science Foundation Plant Genome Grant DBI-0211659, State and Federal Funds appropriated to OARDC, Ohio State University, BASF Plant Sciences, and the Gatsby Charitable Foundation.

Received April 27, 2009; revised August 1, 2009; accepted September 8, 2009; published September 30, 2009.

REFERENCES

Allen, R.L., Bittner-Eddy, P.D., Grenville-Briggs, L.J., Meitz, J.C., Rehmany, A.P., Rose, L.E., and Beynon, J.L. (2004). Host-parasite coevolutionary conflict between Arabidopsis and downy mildew. Science **306:** 1957–1960.

Allen, R.L., Meitz, J.C., Baumber, R.E., Hall, S.A., Lee, S.C., Rose, L.E., and Beynon, J.L. (2008). Natural variation reveals key amino acids in a downy mildew effector that alters recognition specificity by an Arabidopsis resistance gene. Mol. Plant Pathol. **9:** 511–523.

Altschul, S.F., Madden, T.L., Schaffer, A.A., Zhang, J., Zhang, Z., Miller, W., and Lipman, D.J. (1997). Gapped BLAST and PSI-BLAST: A new generation of protein database search programs. Nucleic Acids Res. **25:** 3389–3402.

Anisimova, M., Bielawski, J.P., and Yang, Z. (2001). Accuracy and power of the likelihood ratio test in detecting adaptive molecular evolution. Mol. Biol. Evol. **18:** 1585–1592.

Armstrong, M.R., et al. (2005). An ancestral oomycete locus contains late blight avirulence gene *Avr3a*, encoding a protein that is recognized in the host cytoplasm. Proc. Natl. Acad. Sci. USA **102:** 7766–7771.

Austin, M.J., Muskett, P., Kahn, K., Feys, B.J., Jones, J.D.G., and Parker, J.E. (2002). Regulatory role of SGT1 in early *R* gene-mediated plant defenses. Science **295:** 2077–2080.

Azevedo, C., Sadanandom, A., Kitagawa, K., Freialdenhoven, A., Shirasu, K., and Schulze-Lefert, P. (2002). The RAR1 interactor SGT1, an essential component of *R* gene-triggered disease resistance. Science **295:** 2073–2076.

Ballvora, A., Ercolano, M.R., Weiss, J., Meksem, K., Bormann, C.A., Oberhagemann, P., Salamini, F., and Gebhardt, C. (2002). The *R1* gene for potato resistance to late blight (*Phytophthora infestans*) belongs to the leucine zipper/NBS/LRR class of plant resistance genes. Plant J. **30:** 361–371.

Bhattacharjee, S., Hiller, N.L., Liolios, K., Win, J., Kanneganti, T.D., Young, C., Kamoun, S., and Haldar, K. (2006). The malarial host-targeting signal is conserved in the Irish potato famine pathogen. PLoS Pathog. **2:** e50.

Birch, P.R., Boevink, P.C., Gilroy, E.M., Hein, I., Pritchard, L., and Whisson, S.C. (2008). Oomycete RXLR effectors: Delivery, functional redundancy and durable disease resistance. Curr. Opin. Plant Biol. **11:** 373–379.

Birch, P.R., Rehmany, A.P., Pritchard, L., Kamoun, S., and Beynon, J.L. (2006). Trafficking arms: Oomycete effectors enter host plant cells. Trends Microbiol. **14:** 8–11.

Block, A., Li, G., Fu, Z.Q., and Alfano, J.R. (2008). Phytopathogen type III effector weaponry and their plant targets. Curr. Opin. Plant Biol. **11:** 396–403.

Bos, J.I., Kanneganti, T.D., Young, C., Cakir, C., Huitema, E., Win, J., Armstrong, M.R., Birch, P.R., and Kamoun, S. (2006). The C-terminal half of *Phytophthora infestans* RXLR effector AVR3a is sufficient to trigger R3a-mediated hypersensitivity and suppress INF1-induced cell death in *Nicotiana benthamiana.* Plant J. **48:** 165–176.

Bos, J.I.B., Armstrong, M., Whisson, S.C., Torto, T., Ochwo, M., Birch, P.R.J., and Kamoun, S. (2003). Intraspecific comparative genomics to identify avirulence genes from *Phytophthora.* New Phytol. **159:** 63–72.

Bos, J.I.B., Chaparro-Garcia, A., Quesada-Ocampo, L.M., McSpadden-Gardener, B.B., and Kamoun, S. (2009). Distinct amino acids of the *Phytophthora infestans* effector AVR3a condition activation of R3a hypersensitivity and suppression of cell death. Mol. Plant Microbe Interact. **22:** 269–281.

Catanzariti, A.M., Dodds, P.N., and Ellis, J.G. (2007). Avirulence proteins from haustoria-forming pathogens. FEMS Microbiol. Lett. **269:** 181–188.

Caten, C.E., and Jinks, J.L. (1968). Spontaneous variability of single isolates of *Phytophthora infestans*. I. Cultural variation. Can. J. Bot. **46:** 329–347.

Chenna, R., Sugawara, H., Koike, T., Lopez, R., Gibson, T.J., Higgins, D.G., and Thompson, J.D. (2003). Multiple sequence alignment with the Clustal series of programs. Nucleic Acids Res. **31:** 3497–3500.

Chisholm, S.T., Coaker, G., Day, B., and Staskawicz, B.J. (2006). Host-microbe interactions: Shaping the evolution of the plant immune response. Cell **124:** 803–814.

Cunnac, S., Lindeberg, M., and Collmer, A. (2009). *Pseudomonas syringae* type III secretion system effectors: Repertoires in search of functions. Curr. Opin. Microbiol. **12:** 53–60.

Damasceno, C.M., Bishop, J.G., Ripoll, D.R., Win, J., Kamoun, S., and Rose, J.K. (2008). Structure of the glucanase inhibitor protein (GIP) family from phytophthora species suggests coevolution with plant endo-beta-1,3-glucanases. Mol. Plant Microbe Interact. **21:** 820–830.

Dodds, P.N., Lawrence, G.J., Catanzariti, A.M., Ayliffe, M.A., and Ellis, J.G. (2004). The *Melampsora lini* AvrL567 avirulence genes are expressed in haustoria and their products are recognized inside plant cells. Plant Cell **16:** 755–768.

Dodds, P.N., Lawrence, G.J., Catanzariti, A.M., Teh, T., Wang, C.I., Ayliffe, M.A., Kobe, B., and Ellis, J.G. (2006). Direct protein interaction underlies gene-for-gene specificity and coevolution of the flax resistance genes and flax rust avirulence genes. Proc. Natl. Acad. Sci. USA **103:** 8888–8893.

Dou, D., Kale, S.D., Wang, X., Chen, Y., Wang, Q., Jiang, R.H., Arredondo, F.D., Anderson, R.G., Thakur, P.B., McDowell, J.M., Wang, Y., and Tyler, B.M. (2008b). Conserved C-terminal motifs required for avirulence and suppression of cell death by *Phytophthora sojae* effector Avr1b. Plant Cell **20:** 1118–1133.

Dou, D., Kale, S.D., Wang, X., Jiang, R.H., Bruce, N.A., Arredondo, F.D., Zhang, X., and Tyler, B.M. (2008a). RXLR-mediated entry of *Phytophthora sojae* effector Avr1b into soybean cells does not require pathogen-encoded machinery. Plant Cell **20:** 1930–1947.

Edgar, R.C. (2004). MUSCLE: Multiple sequence alignment with high accuracy and high throughput. Nucleic Acids Res. **32:** 1792–1797.

Eddy, S.R. (1998). Profile hidden Markov models. Bioinformatics **14:** 755–763.

Fry, W.E. (2008). *Phytophthora infestans*: The plant (and *R* gene) destroyer. Mol. Plant Pathol. **9:** 385–402.

Gietz, R.D., Schiestl, R.H., Willems, A.R., and Woods, R.A. (1995). Studies on the transformation of intact yeast cells by the LiAc/SS-DNA/PEG procedure. Yeast **11:** 355–360.

Grouffaud, S., van West, P., Avrova, A.O., Birch, P.R., and Whisson, S.C. (2008). *Plasmodium falciparum* and *Hyaloperonospora parasitica* effector translocation motifs are functional in *Phytophthora infestans.* Microbiology **154:** 3743–3751.

Gurlebeck, D., Jahn, S., Gurlebeck, N., Szczesny, R., Szurek, B., Hahn, S., Hause, G., and Bonas, U. (2009). Visualization of novel virulence activities of the *Xanthomonas* type III effectors AvrBs1, AvrBs3 and AvrBs4. Mol. Plant Pathol. **10:** 175–188.

Guo, M., Tian, F., Wamboldt, Y., and Alfano, J.R. (2009) The majority of the type III effector inventory of *Pseudomonas syringae* pv. *tomato* DC3000 can suppress plant immunity. Mol. Plant Microbe Interact. (in press).

Haas, B., et al. (2009). Genome sequence and comparative analysis of the Irish potato famine pathogen *Phytophthora infestans.* Nature **461:** 393–398.

Halterman, D.A., Colton Kramer, L., Wielgus, S., and Jiang, J. (2008). Performance of transgenic potato containing the late blight resistance gene RB. Plant Dis. **92:** 339–343.

Helgeson, J.P., Pohlman, J.D., Austin, S., Haberlach, G.T., Wielgus, S.M., Ronis, D., Zambolim, L., Tooley, P., Mcgrath, J.M., James, R. V., and Stevenson, W.R. (1998). Somatic hybrids between *Solanum bulbocastanum* and potato: A new source of resistance to late blight. Theor. Appl. Genet. **96:** 738–742.

Hellens, R., Mullineaux, P., and Klee, H. (2000). Technical focus: A guide to Agrobacterium binary Ti vectors. Trends Plant Sci. **5:** 446–451.

Hogenhout, S.A., Van der Hoorn, R.A., Terauchi, R., and Kamoun, S. (2009). Emerging concepts in effector biology of plant-associated organisms. Mol. Plant Microbe Interact. **22:** 115–122.

Huang, S., van der Vossen, E., Kuang, H., Vleeshouwers, V., Zhang, N., Borm, T., van Eck, H., Baker, B., Jacobsen, E., and Visser, R. (2005). Comparative genomics enabled the isolation of the *R3a* late blight resistance gene in potato. Plant J. **42:** 251–261.

Huitema, E., Bos, J.I.B., Tian, M., Win, J., Waugh, M.E., and Kamoun, S. (2004). Linking sequence to phenotype in *Phytophthora* -plant interactions. Trends Microbiol. **12:** 193–200.

Idnurm, A., and Howlett, B.J. (2001). Pathogenicity genes of phytopathogenic fungi. Mol. Plant Pathol. **2:** 241–255.

Jacobs, K.A., et al. (1997). A genetic selection for isolating cDNAs encoding secreted proteins. Gene **198:** 289–296.

Kamoun, S. (2003). Molecular genetics of pathogenic oomycetes. Eukaryot. Cell **2:** 191–199.

Kamoun, S. (2006). A catalogue of the effector secretome of plant pathogenic oomycetes. Annu. Rev. Phytopathol. **44:** 41–60.

Kamoun, S. (2007). Groovy times: Filamentous pathogen effectors revealed. Curr. Opin. Plant Biol. **10:** 358–365.

Kamoun, S., Honee, G., Weide, R., Lauge, R., Kooman-Gersmann, M., de Groot, K., Govers, F., and de Wit, P.J.G.M. (1999b). The fungal gene *Avr9* and the oomycete gene *inf1* confer avirulence to potato virus X on tobacco. Mol. Plant Microbe Interact. **12:** 459–462.

Kamoun, S., Hraber, P., Sobral, B., Nuss, D., and Govers, F. (1999a). Initial assessement of gene diversity for the oomycete pathogen *Phytophthora infestans* based on expressed sequences. Fungal Genet. Biol. **28:** 94–106.

Kamoun, S., and Smart, C.D. (2005). Late blight of potato and tomato in the genomics era. Plant Dis. **89:** 692–699.

Kamoun, S., van West, P., Vleeshouwers, V.G., de Groot, K.E., and Govers, F. (1998). Resistance of *Nicotiana benthamiana* to *Phytophthora infestans* is mediated by the recognition of the elicitor protein INF1. Plant Cell **10:** 1413–1426.

Kamoun, S., Young, M., Glascock, C., and Tyler, B.M. (1993). Extracellular protein elicitors from *Phytophthora*: Host-specificity and induction of resistance to fungal and bacterial phytopathogens. Mol. Plant Microbe Interact. **6:** 15–25.

Kanneganti, T.D., Huitema, E., Cakir, C., and Kamoun, S. (2006). Synergistic interactions of the plant cell death pathways induced by *Phytophthora infestans* Nepl-like protein PiNPP1.1 and INF1 elicitin. Mol. Plant Microbe Interact. **19:** 854–863.

Kjemtrup, S., Nimchuk, Z., and Dangl, J.L. (2000). Effector proteins of phytopathogenic bacteria: Bifunctional signals in virulence and host recognition. Curr. Opin. Microbiol. **3:** 73–78.

Klein, R.D., Gu, Q., Goddard, A., and Rosenthal, A. (1996). Selection for genes encoding secreted proteins and receptors. Proc. Natl. Acad. Sci. USA **93:** 7108–7113.

Kuang, H., et al. (2005). The R1 resistance gene cluster contains three groups of independently evolving, type I R1 homologues and shows substantial structural variation among haplotypes of *Solanum demissum*. Plant J. **44:** 37–51.

Kuhl, J.C., Zarka, K., Coombs, J., Kirk, W.W., and Douches, D.S. (2007). Late blight resistance of RB transgenic potato lines. J. Am. Soc. Hortic. Sci. **132:** 783–789.

Lee, S.J., Kelley, B.S., Damasceno, C.M., St John, B., Kim, B.S., Kim, B.D., and Rose, J.K. (2006). A functional screen to characterize the secretomes of eukaryotic pathogens and their hosts in planta. Mol. Plant Microbe Interact. **19:** 1368–1377.

Lindbo, J.A. (2007). TRBO: A high efficiency *Tobacco mosaic virus* RNA based overexpression vector. Plant Physiol. **145:** 1232–1240.

Liu, Y., Schiff, M., Serino, G., Deng, X.W., and Dinesh-Kumar, S.P. (2002). Role of SCF ubiquitinligase and the COP9 signalosome in the *N* gene-mediated resistance response to *Tobacco mosaic virus.* Plant Cell **14:** 1483–1496.

Liu, Z., Bos, J.I.B., Armstrong, M., Whisson, S.C., da Cunha, L., Torto-Alalibo, T., Win, J., Avrova, A.O., Wright, F., Birch, P.R.J., and Kamoun, S. (2005). Patterns of diversifying selection in the phytotoxin-like *scr74* gene family of *Phytophthora infestans.* Mol. Biol. Evol. **22:** 659–672.

Lu, R., Malcuit, I., Moffett, P., Ruiz, M.T., Peart, J., Wu, A.J., Rathjen, J.P., Bendahmane, A., Day, L., and Baulcombe, D.C. (2003). High throughput virus-induced gene silencing implicates heat shock protein 90 in plant disease resistance. EMBO J. **22:** 5690–5699.

Menne, K.M., Hermjakob, H., and Apweiler, R. (2000). A comparison of signal sequence prediction methods using a test set of signal peptides. Bioinformatics **16:** 741–742.

Moffett, P., Farnham, G., Peart, J., and Baulcombe, D.C. (2002). Interaction between domains of a plant NBS-LRR protein in disease resistance related cell death. EMBO J. **21:** 4511–4519.

Morgan, W., and Kamoun, S. (2007). RXLR effectors of plant pathogenic oomycetes. Curr. Opin. Microbiol. **10:** 332–338.

Nasir, K.H., et al. (2005). High-throughput in planta expression screening identifies a class II ethylene-responsive element binding factor-like protein that regulates plant cell death and non-host resistance. Plant J. **43:** 491–505.

Nei, M., and Gojobori, T. (1986). Simple methods for estimating the numbers of synonymous and nonsynonymous nucleotide substitutions. Mol. Biol. Evol. **3:** 418–426.

Nielsen, H., Engelbrecht, J., Brunak, S., and von Heijne, G. (1997). Identification of prokaryotic and eukaryotic signal peptides and prediction of their cleavage sites. Protein Eng. **10:** 1–6.

Nielsen, R., and Yang, Z. (1998). Likelihood models for detecting positively selected amino acid sites and applications to the HIV-1 envelope gene. Genetics **148:** 929–936.

Nurnberger, T., and Brunner, F. (2002). Innate immunity in plants and animals: Emerging parallels between the recognition of general elicitors and pathogen-associated molecular patterns. Curr. Opin. Plant Biol. **5:** 318–324.

O'Connell, R.J., and Panstruga, R. (2006). Tete a tete inside a plant cell: establishing compatibility between plants and biotrophic fungi and oomycetes. New Phytol. **171:** 699–718.

Peart, J.R., et al. (2002). Ubiquitin ligase-associated protein SGT1 is required for host and nonhost disease resistance in plants. Proc. Natl. Acad. Sci. USA **99:** 10865–10869.

Qutob, D., et al. (2006). Phytotoxicity and innate immune responses induced by NEP1-like proteins. Plant Cell **18:** 3721–3744.

Randall, T.A., et al. (2005). Large-scale gene discovery in the oomycete *Phytophthora infestans* reveals likely components of phytopathogenicity shared with true fungi. Mol. Plant Microbe Interact. **18:** 229–243.

Rehmany, A.P., Gordon, A., Rose, L.E., Allen, R.L., Armstrong, M.R., Whisson, S.C., Kamoun, S., Tyler, B.M., Birch, P.R., and Beynon,

J.L. (2005). Differential recognition of highly divergent downy mildew avirulence gene alleles by *RPP1* resistance genes from two *Arabidopsis* lines. Plant Cell **17:** 1839–1850.

Sambrook, J., and Russell, D.W. (2001). Molecular Cloning: A Laboratory Manual. (Cold Spring Harbor, NY: Cold Spring Harbor Laboratory).

Schneider, G., and Fechner, U. (2004). Advances in the prediction of protein targeting signals. Proteomics **4:** 1571–1580.

Song, J., Bradeen, J.M., Naess, S.K., Raasch, J.A., Wielgus, S.M., Haberlach, G.T., Liu, J., Kuang, H., Austin-Phillips, S., Buell, C.R., Helgeson, J.P., and Jiang, J. (2003). Gene RB cloned from *Solanum bulbocastanum* confers broad spectrum resistance to potato late blight. Proc. Natl. Acad. Sci. USA **100:** 9128–9133.

Takahashi, Y., Nasir, K.H., Ito, A., Kanzaki, H., Matsumura, H., Saitoh, H., Fujisawa, S., Kamoun, S., and Terauchi, R. (2007). A high-throughput screen of cell-death-inducing factors in *Nicotiana benthamiana* identifies a novel MAPKK that mediates INF1-induced cell death signaling and non-host resistance to *Pseudomonas cichorii.* Plant J. **49:** 1030–1040.

Takken, F.L., Luderer, R., Gabriels, S.H., Westerink, N., Lu, R., De Wit, P.J., and Joosten, M.H. (2000). A functional cloning strategy, based on a binary PVX expression vector, to isolate HR-inducing cDNAs of plant pathogens. Plant J. **24:** 275–283.

Talbot, N.J. (2003). On the trail of a cereal killer: Exploring the biology of *Magnaporthe grisea.* Annu. Rev. Microbiol. **57:** 177–202.

Thomas, J.H. (2006). Adaptive evolution in two large families of ubiquitin-ligase adapters in nematodes and plants. Genome Res. **16:** 1017–1030.

Tian, M., Benedetti, B., and Kamoun, S. (2005). A Second Kazal-like protease inhibitor from *Phytophthora infestans* inhibits and interacts with the apoplastic pathogenesis-related protease P69B of tomato. Plant Physiol. **138:** 1785–1793.

Tian, M., Huitema, E., da Cunha, L., Torto-Alalibo, T., and Kamoun, S. (2004). A Kazal-like extracellular serine protease inhibitor from *Phytophthora infestans* targets the tomato pathogenesis-related protease P69B. J. Biol. Chem. **279:** 26370–26377.

Tian, M., Win, J., Song, J., van der Hoorn, R., van der Knaap, E., and Kamoun, S. (2007). A *Phytophthora infestans* cystatin-like protein targets a novel tomato papain-like apoplastic protease. Plant Physiol. **143:** 364–377.

Torto, T., Li, S., Styer, A., Huitema, E., Testa, A., Gow, N.A.R., van West, P., and Kamoun, S. (2003). EST mining and functional expression assays identify extracellular effector proteins from *Phytophthora.* Genome Res. **13:** 1675–1685.

Torto, T.A., Rauser, L., and Kamoun, S. (2002). The *pipg1* gene of the oomycete *Phytophthora infestans* encodes a fungal-like endopolygalacturonase. Curr. Genet. **40:** 385–390.

Tyler, B.M., et al. (2006). *Phytophthora* genome sequences uncover evolutionary origins and mechanisms of pathogenesis. Science **313:** 1261–1266.

Van der Hoorn, R.A.L., and Kamoun, S. (2008). From guard to decoy: A new model for perception of plant pathogen effectors. Plant Cell **20:** 2009–2017.

Van der Hoorn, R.A., Laurent, F., Roth, R., and De Wit, P.J. (2000). Agroinfiltration is a versatile tool that facilitates comparative analyses of *Avr9*/*Cf-9*-induced and *Avr4*/*Cf-4*-induced necrosis. Mol. Plant Microbe Interact. **13:** 439–446.

van der Vossen, E., Sikkema, A., Hekkert, B.L., Gros, J., Stevens, P., Muskens, M., Wouters, D., Pereira, A., Stiekema, W., and Allefs, S. (2003). An ancient *R* gene from the wild potato species *Solanum bulbocastanum* confers broad-spectrum resistance to *Phytophthora infestans* in cultivated potato and tomato. Plant J. **36:** 867–882.

van der Vossen, E.A., Gros, J., Sikkema, A., Muskens, M., Wouters, D., Wolters, P., Pereira, A., and Allefs, S. (2005). The *Rpi-blb2* gene from *Solanum bulbocastanum* is an *Mi-1* gene homolog conferring broad-spectrum late blight resistance in potato. Plant J. **44:** 208–222.

van Poppel, P.M., Guo, J., van de Vondervoort, P.J., Jung, M.W., Birch, P.R., Whisson, S.C., and Govers, F. (2008). The *Phytophthora infestans* avirulence gene *Avr4* encodes an RXLR-dEER effector. Mol. Plant Microbe Interact. **21:** 1460–1470.

Vleeshouwers, V.G., et al. (2008). Effector genomics accelerates discovery and functional profiling of potato disease resistance and *Phytophthora infestans* avirulence genes. PLoS One **3:** e2875.

Vleeshouwers, V.G.A.A., Driesprong, J.-D., Kamphuis, L.G., Torto-Alalibo, T., van 't Slot, K.A.E., Govers, F., Visser, R.G.F., Jacobsen, E., and Kamoun, S. (2006). Agroinfection-based high throughput screening reveals specific recognition of INF elicitins in *Solanum.* Mol. Plant Pathol. **7:** 499–510.

Voinnet, O., Rivas, S., Mestre, P., and Baulcombe, D. (2003). An enhanced transient expression system in plants based on suppression of gene silencing by the p19 protein of tomato bushy stunt virus. Plant J. **33:** 949–956.

Wang, M., Allefs, S., van den Berg, R.G., Vleeshouwers, V.G., van der Vossen, E.A., and Vosman, B. (2008). Allele mining in *Solanum*: Conserved homologues of *Rpi-blb1* are identified in *Solanum stoloniferum.* Theor. Appl. Genet. **116:** 933–943.

Whisson, S.C., et al. (2007). A translocation signal for delivery of oomycete effector proteins into host plant cells. Nature **450:** 115–118.

Win, J., Kanneganti, T.D., Torto-Alalibo, T., and Kamoun, S. (2006). Computational and comparative analyses of 150 full-length cDNA sequences from the oomycete plant pathogen *Phytophthora infestans.* Fungal Genet. Biol. **43:** 20–33.

Win, J., Morgan, W., Bos, J., Krasileva, K.V., Cano, L.M., Chaparro-Garcia, A., Ammar, R., Staskawicz, B.J., and Kamoun, S. (2007). Adaptive evolution has targeted the C-terminal domain of the RXLR effectors of plant pathogenic oomycetes. Plant Cell **19:** 2349–2369.

Wroblewski, T., et al. (2009). Comparative large-scale analysis of interactions between several crop species and the effector repertoires from multiple pathovars of *Pseudomonas* and *Ralstonia.* Plant Physiol. **150:** 1733–1749.

Yang, Z. (2007). PAML 4: Phylogenetic analysis by maximum likelihood. Mol. Biol. Evol. **24:** 1586–1591.

Yang, Z., and Nielsen, R. (2000). Estimating synonymous and nonsynonymous substitution rates under realistic evolutionary models. Mol. Biol. Evol. **17:** 32–43.

Yang, Z., Nielsen, R., Goldman, N., and Pedersen, A.M. (2000). Codon-substitution models for heterogeneous selection pressure at amino acid sites. Genetics **155:** 431–449.

Yang, Z., Wong, W.S., and Nielsen, R. (2005). Bayes empirical bayes inference of amino acid sites under positive selection. Mol. Biol. Evol. **22:** 1107–1118.